LINEAR QUADRATIC CONTROL FOR SYSTEMS WITH STRUCTURED UNCERTAINTY

by

Joel S. Douglas

B.S., Electrical Engineering, Carnegie Mellon University
(1989)

Submitted to the Department of Electrical Engineering and Computer Science
in partial fulfillment of the requirements for the degree of

MASTER OF SCIENCE

at the

MASSACHUSETTS INSTITUTE OF TECHNOLOGY

May 1991

Signature of Author.....
Department of Electrical Engineering and Computer Science
May 24, 1991

Certified by.....
Michael Athans
Professor of Electrical Engineering
Thesis Supervisor

Certified by.....
Andreas von Flotow
Associate Professor of Aeronautics and Astronautics
Thesis Co-supervisor

Accepted by.....
Arthur C. Smith
Chair, Department Committee on Graduate Students

LINEAR QUADRATIC CONTROL FOR SYSTEMS WITH STRUCTURED UNCERTAINTY

by

Joel S. Douglas

Submitted to the Department of Electrical Engineering and Computer Science
on May 24, 1991, in partial fulfillment of the requirements for the degree of
MASTER OF SCIENCE

Abstract

The standard LQR design technique is extended to systems with parametric uncertainty in the open-loop "A" matrix. This design, called the robust LQR (RLQR), guarantees the stability of the uncertain system, and the same level of performance robustness as standard LQR designs.

To determine the properties of the RLQR design, simulations are performed on various mass-spring systems, and compared to a mismatched LQR controller, designed on the "nominal" system. These simulations show the RLQR design first reduces the length of the uncertain springs to their equilibrium value, so as to mitigate their effect on the dynamics of the system, and then regulates the system to the zero position. Additional control variables increase the performance robustness of the design. Simulations also show that disturbances are attenuated, even better than in the mismatched LQR design.

The RLQR design differs from the standard LQR design in that two additional terms are added to the standard LQR cost functional. The first is interpreted as a weighted sum of the uncertain stored potential energies of the springs. The second is equivalent to a "worst-case" disturbance in the direction of the parametric uncertainty. We then show these interpretations hold in general structural systems with uncertain stiffness and damping matrices.

We show that we are guaranteed better performance robustness than the mismatched LQR design. The price we pay is less robustness to high-frequency unstructured uncertainty. Also, we show that the design is conservative with respect to stability robustness.

Thesis Supervisor: Michael Athans, Professor of Electrical Engineering
Thesis Co-supervisor: Andreas von Flotow, Associate Professor of Aeronautics and Astronautics

Acknowledgments

I would like to thank my thesis supervisor, Professor Michael Athans, for his help and guidance over these last two years. He has helped direct me in my work, and shown the importance of my results in the "big picture." Professor Athans has also helped teach me how to properly present my work, both in oral presentations and on paper.

I would also like to thank my thesis co-supervisor, Professor Andreas von Flotow, for his willingness to dedicate his time to my work on short notice.

There are many other people who have offered me their technical guidance during this research. These include Professor Armando Rodriguez, who has been both my advisor and my friend; Douglas MacMartin, who helped me understand power dissipation in structural systems, and Leonard Lublin, who has helped me understand various aspects of structural systems; Dr. Daniel Miller, who has helped with various proofs; Dr. Dragan Obradovic and Ignacio Diaz-Bobillo, who have helped me better understand control theory.

I would also like to thank the various friends I have made over these past two years. I would especially like to thank my officemate, John Wissinger, who has kept me inpired about research.

The completion of this thesis marks my twentieth consecutive year in school. Therefore, I would like to dedicate this thesis to the students in my family.

This research was carried out at the MIT Space Engineering Research Center with support from NASA Grant NAGW-1335 from NASA, Washington, D.C., with Mr. Samuel Venneri serving as technical monitor.

Contents

Chapter 1

Introduction

In this chapter, we will define structured uncertainty, and motivate the need for controlling systems with such uncertainty. A brief summary of some of the previous work in this area will be presented, and then we will state what this thesis adds to the field.

1.1 Motivation

Systems to be controlled have some inherent uncertainty in their models. This typically arises from modeling errors or the inability to precisely quantify certain parameters. This uncertainty comes in two basic flavors: unstructured and structured uncertainty. The former is typically the high frequency uncertainty which we account for by rolling off the compensator. Structured uncertainty includes parametric uncertainty, and is to be the type of uncertainty considered in this thesis.

A typical example of a system with both types of uncertainty is a large space structure. We know that the system is open-loop stable; that is if we don't apply any controls the structure should not fall apart. But in order to achieve our performance goals we typically have to control the system very accurately. A typical large space structure is a very flexible system, and thus is hard to model and control. Certain parameters, such

as damping and stiffness coefficients, may only be known within a given range. Also, precise knowledge of high frequency dynamics is not available. Methods of controlling such a system need to be developed.

This thesis will consider a first step in understanding how to control systems with structured parametric uncertainty. An extension of the standard linear quadratic regulator (LQR) design will be proposed for systems with certain types of parametric uncertainty. This design will guarantee the stability of the closed-loop system, and also provide some additional robustness guarantees. This can only be considered a first step in the evolution of a robust design methodology because perfect knowledge of all states must be assumed.

A major portion of this work will be devoted to understanding how such a robust controller achieves its goal, using a combination of analysis and simulations. Though, as shown in section 1.2, there have been a number of control designs for systems with structured uncertainty proposed, an understanding of the basic nature of these robust controllers is still lacking. By examining how the energy changes in an uncertain system with a robust controller, a better understanding of how to design for parametric uncertainty will be obtained. Thus, several simulations will be carried out so that the changes in energy can be observed.

1.2 Background

Many tools exist for the analysis of systems with parameter uncertainty. Probably the most basic is Kharitonov's Theorem [3]. Given a polynomial where all of the coefficients can vary independently in prescribed ranges, the stability of the polynomial can be deduced from the stability of only four polynomials. These four polynomials correspond to those in the unknown set with the maximum or minimum imaginary parts, and the maximum or minimum real parts. An elementary proof is shown in [21].

This theorem, though quite restrictive, initiated much research into the analysis of

systems with structured uncertainty. Most notable is the work of Barmish [2, 3], who extended the results of Kharitonov to include dependent variations in coefficients, and Petersen [26, 27] who extended the results to include more general stability regions than the left half plane, and also extended the theorem to include more general families of polynomials. Dasgupta [11] extended the results for systems under nonlinear passive feedback. Chappellat and Bhattacharyya [10] also extended Kharitonov's results to "interval plants". Another major contribution was the work of Bartlett, Hollot, and Lin [5], who proved the following "Edge Theorem": the stability of a polytope of polynomials can be determined by checking the exposed edges of that polytope.

Many other techniques exist for the analysis of uncertain systems. To determine the closed-loop poles of an uncertain system, Barmish created the "Robust Root Locus" [4], which is a technique for generating the root loci of a feedback system with perturbations. Mansour [20] examined the stability of interval matrices, which is a more difficult problem than the stability of interval polynomials.

While all of this work is very important, it has the drawback that it can be used only for the analysis of uncertain systems. Designing controllers for systems with structured uncertainty is a much more difficult task.

Some simple schemes for designing controllers for uncertain systems have been proposed. Hollot and Yang [18] presented necessary and sufficient conditions for a lead or lag compensator to robustly stabilize a family of interval plants. Wei and Barmish [32] presented a simple recipe to determine feedback gains to make a polynomial Hurwitz invariant.

Many of the approaches involve finding gains which will "simultaneously stabilize" a family of polynomials. For an example, see [17], in which the problem of stabilizing a plant with an interval denominator and right half plane zeros is reduced to finding a compensator which simultaneously stabilizes four plants. This is one example of an application of Kharitonov's Theorem.

Another algorithm for stabilizing controllers with structural uncertainties was pro-

posed by Wei [31]. This algorithm allows for time-varying uncertainties. A stabilizing method is proposed, and necessary and sufficient conditions are given for when a system can be quadratically stabilized.

One of the major contributions in the area of design for uncertain systems is the work by Petersen, [23, 24, 25], who has used Lyapunov methods to design a stabilizing controller for an uncertain system by solving a single Riccati-like equation. It relies on a method called the "Petersen-Hollot bound" [28], which is a method of overbounding a set of Lyapunov equations. The Petersen-Hollot bound approach has been followed in many other works, this research included.

Other work using the overbounding approach is Bernstein's "Optimal Projection for Uncertain Systems." In a series of papers, Bernstein uses an overbounding procedure to extend the standard LQG theory to design a controller of a fixed (i.e. reduced) order, and robust to parameter uncertainty. The result is a single design methodology which requires the solution of two Riccati equations and two Lyapunov equations which are coupled. Some of Bernstein's relevant works are [8], [7], [13], [14], [15], and [16]; see [9] for an overview of the philosophy behind the work. Also see [6] for a comparison between deterministic and stochastic methods for determining a robust controller, and their application to Petersen-Hollot bounds. Our work will involve taking a small subset of these optimal projection equations (i.e. full order controllers with full-state feedback), and examining them in close detail to determine their properties, and the underlying fundamentals behind this method of robust control for parametric uncertainty.

Although we can see from this small sampling that much work has been done in the design of controllers for systems with parametric uncertainty, much more work needs to be done before we can really understand how to design such a robust controller.

1.3 Contributions of Thesis

This thesis will present a robust linear quadratic regulator, or RLQR, which is robust to parametric uncertainty. The design relies on overbounding a set of equations, in the same manner as Petersen [28]. In fact, as stated earlier, we use the overbounding method proposed by Petersen called the Petersen-Hollot bounds in order to guarantee performance-robustness of the uncertain system. The resulting controller is determined by the solution of a Riccati-like equation, which has appeared in the literature.

Thus, the primary contribution of this thesis is not the novelty of the design equations. Rather, it is the new perspective from which they are derived, as a direct extension of LQR to a controller with certain guaranteed robustness for all parameter variations. Even more importantly, this thesis tries to expose what are the underlying fundamentals necessary to robustify a system to this type of uncertainty, including how a system compensates for uncertain parameters, and the impact of additional control variables on performance robustness. Several simulations are presented, which show certain intriguing (and initially unexpected) properties of the design procedure. Then several novel interpretations are made using energy and power uncertainty arguments, which help explain what physical properties of the controller make it robust. This "uncertain energy" interpretation is shown to hold for more general structural systems, with uncertain stiffness and damping matrices.

The hope is that our results will provide a deeper understanding of the necessary ingredients of a robust design. This will guide us in our future work in "robustifying" more general controllers not considered in this thesis, such as controllers which do not rely on full-state feedback.

1.4 Outline

The technical details of designing the robust LQR (RLQR) method is presented in Chapter 2. First, we will review the standard classical LQR results, which is the optimal

design on a system without uncertainty. Then we will extend the LQR equations to account for parametric uncertainty.

To observe the behavior of the RLQR controller, several simulations are presented in Chapter 3. We will start with a simple "benchmark" problem involving two masses connected by an uncertain spring, and then examine some more complicated mass-spring systems to compare the RLQR design to a design where we choose feedback gains based on an LQR design of the "nominal" system.

Chapter 4 will provide an analytical framework for examining these RLQR properties. It is in this chapter where we provide the interesting energy related interpretations of the robust design properties and structure of the equations. The energy interpretations are extended for general structural systems, with uncertain stiffness and damping matrices.

Finally, Chapter 5 will summarize our main conclusions, and show the directions for future research.

Chapter 2

Extension of LQR

In this chapter, we will extend the standard LQR methodology to account for parametric uncertainty. First we will state the LQR results, and show that they do not guarantee stability in the case of parametric uncertainty. Then we will derive a new version of LQR which is robust to this uncertainty, provided that a solution to a Riccati-like equation exists.

2.1 Uncertain System

We assume we have an uncertain linear system of the form

$$\dot{x}(t) = Ax(t) + Bu(t) \tag{2.1}$$

We will study the case when there are uncertain, but constant, parameters. We will further assume that all the uncertainty is in the "A" matrix. This is typical of large space structures, where stiffness and damping coefficients which appear in the "A" matrix are not known well, but values such as masses, which also influence the "B" matrix, are known with a greater degree of accuracy.

We model the uncertain A matrix in the form

$$A = A_0 + \sum_{i=1}^{p} q_i E_i \quad |q_i| \leq 1 \tag{2.2}$$

$$E_i = l_i n_i^T \tag{2.3}$$

where A_0 represents the "nominal" system, and each uncertain constant parameter is known to be in a bounded interval; we assume we have p uncertain parameters. The E_i matrices represent the structure of the uncertainty, and are scaled so that the magnitudes of the scalars q_i are less than 1. We further assume that the rank of each E_i is equal to 1. The implications of this assumption will be discussed in section 4.5.2.

We assume we have exact measurement of all states for the purpose of feedback. Though this may not be realistic in real structures, understanding the underlying fundamentals in this framework will help direct us when we assume knowledge of only the output variables.

2.2 Mismatched LQR

2.2.1 Optimal Regulator

The Linear Quadratic Regulator (LQR) is the optimal regulator for systems without uncertainty. It is optimal in that it minimizes the cost functional given by

$$J = \int_0^\infty (x^T(t)Qx(t) + \rho u^T(t)u(t))dt \tag{2.4}$$

where $Q = Q^T \geq 0$ is the state-weighting matrix, and $\rho > 0$ is the scalar control weighting. We now summarize the LQR results. For more detailed explanations, see [19].

Let us assume we have a system of the form

$$\dot{x}(t) = A_0 x(t) + Bu(t) \tag{2.5}$$

Let us further assume that $[A_0, B]$ is stabilizable and $[A_0, N]$ is detectable, where $Q = N^T N$ for some matrix N (N exists since $Q \geq 0$). Notice that both these assumptions hold in a structural system, which is inherently open-loop stable.

Given these assumptions, then the "optimal" controller is given by

$$u(t) = -Gx(t) \tag{2.6}$$

where

$$G = \frac{1}{\rho} B^T P \tag{2.7}$$

and $P = P^T > 0$ is computed from the standard algebraic Riccati equation

$$-PA_0 - A_0^T P - Q + \frac{1}{\rho} PBB^T P = 0 \tag{2.8}$$

Here, G is the feedback gain matrix. The loop transfer function can be shaped by the choice of Q and ρ. For a discussion of loop shaping via these parameters, see [1].

2.2.2 Applying LQR to Uncertain Systems

Classical LQR designs have some inherent robustness properties. Specifically, we are guaranteed an infinite upwards gain margin, a downwards gain margin of .5, and a phase margin of $\pm 60°$ in each control channel independently and simulateously [29]. Thus, it may be tempting to conjecture (as we did) that the linear quadratic regulator is somehow robust to parametric uncertainty. However, this is not so. We have shown that "blindly" designing an LQR controller on some nominal system does not guarantee the stability of the actual system, even if the actual system is guaranteed to be open-loop stable. An example of this is shown in Appendix A.

We would like to adapt LQR so that we have robustness to parametric uncertainty. Additionally, we would like to retain the robustness properties inherent in the LQR designs, so that we will have limited robustness to unstructured uncertainty. The derivation of this "robust LQR" is given in the next section.

2.3 Robust LQR (RLQR)

2.3.1 Frequency Domain Equality

We want to derive a multi-input multi-output (MIMO) LQR controller which is robust to parametric uncertainty. One way to do this would be to look at Nyquist plots of the uncertain system, and see if we can "bound" the uncertainty in the complex plane. It turns out that this is a difficult thing to do. What is possible, however, is to get an expression for the return difference function, which is the key to the Nyquist plot, in terms of the LQR design parameters. This will help guide us in "robustifying" the LQR design.

The remainder of this section is a derivation of such a frequency domain equation, valid for MIMO designs. In the next section, we will show how this expression will lead us to a robust controller. Then, in section 2.3.3, the robust controller will be derived from the frequency domain equality.

We begin the derivation by repeating the LQR Riccati equation (2.8):

$$-PA_0 - A_0^T P - Q + \frac{1}{\rho} PBB^T P = 0 \tag{2.9}$$

We notice here that we are designing a controller for the nominal system matrix A_0. To account for the uncertainty, we will add and subtract $PA + A^T P$, where A is the unknown (but constant) matrix. We also add and subtract sIP (where s is the frequency domain

variable) and rearrange to get

$$P(sI - A) - (sI + A^T)P + P(A - A_0) + (A^T - A_0^T)P - Q + \frac{1}{\rho}PBB^TP = 0 \qquad (2.10)$$

We now postmultiply both sides of the equation by $(sI - A)^{-1}B$:

$$PB - (sI + A^T)P(sI - A)^{-1}B + P(A - A_0)(sI - A)^{-1}B$$

$$+ (A^T - A_0^T)P(sI - A)^{-1}B - Q(sI - A)^{-1}B + \frac{1}{\rho}PBB^TP(sI - A)^{-1}B = 0 \qquad (2.11)$$

Similarly, we premultiply by $B^T(-sI - A^T)^{-1}$:

$$B^T(-sI - A^T)^{-1}PB + B^TP(sI - A)^{-1}B + B^T(-sI - A^T)^{-1}P(A - A_0)(sI - A)^{-1}B$$

$$+B^T(-sI - A^T)^{-1}(A^T - A_0^T)P(sI - A)^{-1}B - B^T(-sI - A^T)^{-1}Q(sI - A)^{-1}B$$

$$+ B^T(-sI - A^T)^{-1}\frac{1}{\rho}PBB^TP(sI - A)^{-1}B = 0 \qquad (2.12)$$

For more compact notation, we make the following definitions:

$$\Phi(s) = (sI - A)^{-1}, \qquad \Phi^T(-s) = (-sI - A^T)^{-1} \qquad (2.13)$$

$$G = \frac{1}{\rho}B^TP, \qquad \rho G = B^TP, \qquad G^T\rho = PB \qquad (2.14)$$

and thus our equation becomes:

$$B^T\Phi^T(-s)G^T\rho + \rho G\Phi(s)B + B^T\Phi^T(-s)[P(A - A_0) + (A^T - A_0^T)P - Q]\Phi(s)B$$

$$+ B^T\Phi^T(-s)G^T\rho G\Phi(s)B = 0 \qquad (2.15)$$

We rearrange terms to get:

$$\rho I + B^T\Phi^T(-s)G^T\rho + \rho G\Phi(s)B + B^T\Phi^T(-s)G^T\rho G\Phi(s)B$$

$$= \rho I + B^T\Phi^T(-s)[P(A_0 - A) + (A_0^T - A^T)P + Q]\Phi(s)B \tag{2.16}$$

or equivalently:

$$[I+G\Phi(-s)B]^T[I+G\Phi(s)B] = I+\frac{1}{\rho}B^T\Phi^T(-s)[P(A_0-A)+(A_0^T-A^T)P+Q]\Phi(s)B \tag{2.17}$$

This is called the Robust FDE (RFDE), and is the main result of this section. Since G is the set of feedback gains in LQR, this is a frequency domain relation for the actual return difference transfer function matrix $I+G\Phi(s)B$. This is significant because it gives insight into how the Nyquist plot varies in the complex plane for different values of the A matrix.

2.3.2 Method of Robustness

From the RFDE (2.17), it is clear that if

$$P(A_0 - A) + (A_0^T - A^T)P + Q \geq 0 \tag{2.18}$$

then we know that

$$P(A_0 - A) + (A_0^T - A^T)P + Q = F^TF \tag{2.19}$$

for some matrix F. Then it is clear, if we define $G_{LQR} = G\Phi(s)B$, that

$$\sigma_i[I + G_{LQR}(s)] = \sqrt{1 + \sigma_i[F\Phi(s)B]} \tag{2.20}$$

where $\Phi(s) = (sI - A)^{-1}$ as before.

This will guarantee the same robustness as LQR designs on certain systems described earlier in terms of MIMO gain and phase margins. In the complex plane for SISO systems, the expression states that the Nyquist plot of the uncertain system remains

outside the unit disc centered at the critical point. Thus, we will acquire a certain level of robustness to unstructured uncertainty as well as stability and performance robustness to the parametric uncertainty.

2.3.3 RLQR Riccati Equation

Having given the motivation and philosphy behind the robust controller, we will now derive a Riccati Equation which guarantees (2.18). We will use a method known as the Petersen-Hollot bounds [28]. The resulting controller will be called the "Robust LQR", or "RLQR" design.

We start by substituting the standard Riccati equation for the nominal system into equation (2.18). We want to find a value for Q which guarantees the bound, now given by:

$$-PA - A^TP + \frac{1}{\rho}PBB^TP \geq 0 \tag{2.21}$$

We substitute in the actual value of the A matrix (c.f. equations (2.2), (2.3)):

$$A = A_0 + \sum_{i=1}^{p} q_i E_i \tag{2.22}$$

to get

$$-PA_0 - A_0^TP - \sum_{i=1}^{p} q_i PE_i - \sum_{i=1}^{p} q_i E_i^TP + \frac{1}{\rho}PBB^TP \geq 0 \tag{2.23}$$

We know that the inequality (2.23) is true if and only if

$$x^T(-PA_0 - A_0^TP + \frac{1}{\rho}PBB^TP)x - \sum_{i=1}^{p} q_i x^TPE_ix - \sum_{i=1}^{p} q_i x^TE_i^TPx \geq 0 \quad \forall x \in \mathcal{R}^n \tag{2.24}$$

Because $|q_i| \leq 1$, we know we can guarantee the inequality (2.24) if

$$x^T(-PA_0 - A_0^TP + \frac{1}{\rho}PBB^TP)x - 2\sum_{i=1}^{p} |x^TPE_ix| \geq 0 \quad \forall x \in \mathcal{R}^n \tag{2.25}$$

Since we assumed that the matrix E_i is rank 1, we can substitute

$$E_i = l_i n_i^T \tag{2.26}$$

to obtain

$$x^T(-PA_0 - A_0^T P + \frac{1}{\rho} PBB^T P)x - 2\sum_{i=1}^{p} |x^T P l_i n_i^T x| \geq 0 \quad \forall x \in \mathcal{R}^n \tag{2.27}$$

This is guaranteed to be true if

$$x^T(-PA_0 - A_0^T P + \frac{1}{\rho} PBB^T P)x - \sum_{i=1}^{p} \frac{1}{\gamma} x^T P l_i l_i^T P x - \sum_{i=1}^{p} \gamma x^T n_i n_i^T x \geq 0 \quad \forall x \in \mathcal{R}^n \tag{2.28}$$

where we have used the well known inequality $2|ab| \leq \gamma a^2 + \frac{1}{\gamma} b^2$, with γ an arbitrary positive constant.

Let us make the following definitions:

$$L = [l_1\ l_2\ l_3 \ldots]; \qquad N = [n_1\ n_2\ n_3 \ldots] \tag{2.29}$$

Hence our inequality now becomes

$$x^T(-PA_0 - A_0^T P + \frac{1}{\rho} PBB^T P)x - \frac{1}{\gamma} x^T PLL^T Px - \gamma x^T NN^T x \geq 0 \quad \forall x \in \mathcal{R}^n \tag{2.30}$$

This is guaranteed to be satisfied if

$$x^T(-PA_0 - A_0^T P + \frac{1}{\rho} PBB^T P - Q_0 - \frac{1}{\gamma} PLL^T P - \gamma NN^T)x = 0 \quad \forall x \in \mathcal{R}^n \tag{2.31}$$

where Q_0 is some desired state weighting matrix, i.e. the state weighting matrix we would use on the nominal system if there were no uncertainty. An equivalent statement is

$$PA_0 + A_0^T P + (Q_0 + \gamma NN^T) - P(\frac{1}{\rho} BB^T - \frac{1}{\gamma} LL^T)P = 0 \tag{2.32}$$

Thus to design a controller to guarantee stability and robustness, we need to find the solution P to this modified Riccati equation (2.32). Similar Riccati equations have appeared in the literature; for example, see [23]. This reference discusses sufficient conditions for this type of Riccati equation to have a solution.

2.4 Summary

In this chapter, we have derived a controller which is robust to parametric uncertainty. To summarize the methodology, assume the system is of the form

$$\dot{x}(t) = Ax(t) + Bu(t) \tag{2.33}$$

$$A = A_0 + \sum_{i=1}^{p} q_i E_i \quad |q_i| \leq 1 \tag{2.34}$$

$$E_i = l_i n_i^T \tag{2.35}$$

$$L = [l_1\ l_2\ l_3 \ldots]; \qquad N = [n_1\ n_2\ n_3 \ldots] \tag{2.36}$$

The full state controller is defined by

$$u(t) = -Gx(t) \qquad G = \frac{1}{\rho} B^T P \tag{2.37}$$

where G is the constant control matrix and $P = P^T > 0$ is computed from the modified algebraic Riccati equation

$$PA_0 + A_0^T P + (Q_0 + \gamma NN^T) - P(\frac{1}{\rho} BB^T - \frac{1}{\gamma} LL^T)P = 0 \tag{2.38}$$

Here γ is an arbitrary constant. In section 4.3, we will show that not only does γ help control the bandwidth of the system, but it also plays the role of a trade-off parameter between the two terms γNN^T and $\frac{1}{\gamma} LL^T$, which add robustness to the system.

If such a solution P exists, then in addition to guaranteed stability, we are also provid-

ing a certain level of robustness to unstructured uncertainty in terms of gain margins and phase margins. Also, in view of (2.20), we should expect a certain degree of performance robustness.

We now wish to determine some of the properties of the RLQR controller. Instead of jumping into a mathematical derivation, the next chapter will motivate its properties through the use of simulations. Then the properties are explored in an analytical framework in Chapter 4.

Chapter 3

Simulations

In this chapter, we will examine the behavior of the RLQR controller through the use of simulations. We will compare the RLQR controller to a standard LQR design. Interesting behavior of the controller in a simple "benchmark problem" is shown, and then shown to hold true in other systems.

In the simulations, plots will contain either the output variable for various values of the uncertain parameter(s), or typical transients of all state variables for a particular choice of uncertain parameters. The former is shown when we wish to see how the controllers act under different dynamic conditions, and the latter is shown when we wish to see the details of how the closed-loop design performs.

3.1 Benchmark Problem

3.1.1 Original System

Our initial simulations will be performed on the benchmark problem proposed by Wei and Bernstein [30], shown in figure 3-1. Here, two unit masses are coupled by a spring with uncertain stiffness $k \in [.5, 2]$. We wish to control the position $y(t)$ of the second mass by exerting a control force $u(t)$ on the first mass.

This system is representative of dynamical systems with uncertain modal frequencies,

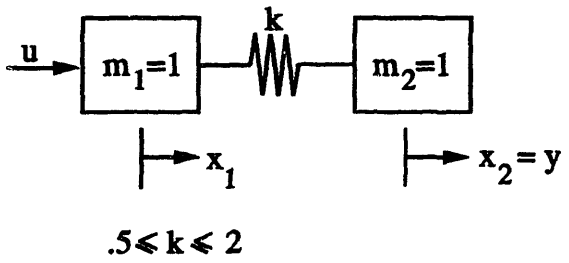

Figure 3-1: The Structure of the Benchmark problem, [30]

and thus is a good starting point for examining the behavior of our controller. Though the system is a simple one, interesting interpretations of the behavior of the system will allow us to understand the behavior of the RLQR controller on more complicated systems.

The system can be written as $\dot{x} = Ax + Bu$, with the values

$$x = \begin{bmatrix} x_1 \\ x_2 \\ x_3 \\ x_4 \end{bmatrix} \qquad A = \begin{bmatrix} 0 & 0 & 1 & 0 \\ 0 & 0 & 0 & 1 \\ -k & k & 0 & 0 \\ k & -k & 0 & 0 \end{bmatrix} \qquad B = \begin{bmatrix} 0 \\ 0 \\ 1 \\ 0 \end{bmatrix} \tag{3.1}$$

where x_1 and x_2 are the positions shown in figure 3-1, and x_3 and x_4 are their respective derivatives (velocities). The open loop poles of this system are

$$\lambda_i = 0, 0, \pm j\sqrt{2k} \tag{3.2}$$

From a physical viewpoint, the potential energy stored in the spring is $\frac{1}{2}k(x_1 - x_2)^2$. Hence, the uncertainty in the spring stiffness implies uncertainty in the stored potential energy. Since both masses are known, there is no uncertainty in the kinetic energy.

As a basis for comparison, we designed a standard LQR control for the nominal system, characterized by the midpoint value $k = 1.25$, and applied the control to the

system with different values of the spring constant. The nominal design parameters were

$$\rho = .01 \qquad Q_0 = \begin{bmatrix} 0 & 0 & 0 & 0 \\ 0 & 1 & 0 & 0 \\ 0 & 0 & 0 & 0 \\ 0 & 0 & 0 & 0 \end{bmatrix} \tag{3.3}$$

This choice of Q_0 implies that our main performance objective is the output transient $y(t) = x_2(t)$. The resulting control gain and closed loop poles are shown in Appendix B.1.

The output transients are shown in figure 3-2. The plot where $k = 1.25$ is the nominal system for which we designed the control and computed the LQR gain, whereas the control is mismatched in the other plots.

Note from figure 3-2 that the transient response can vary widely depending on the actual value of the spring. The "differences" in the shape of the transient responses are an indication of the "performance unrobustness" in this numerical example and are the consequences of the wide variation of potential energy among the mismatched designs. In this example, the system always remains stable, although this is not guaranteed in mismatched classical LQR designs, as was shown in Appendix A.

To apply the RLQR controller, we wrote the uncertain A matrix as (c.f. eq. (2.2))

$$A = \begin{bmatrix} 0 & 0 & 1 & 0 \\ 0 & 0 & 0 & 1 \\ -1.25 & 1.25 & 0 & 0 \\ 1.25 & -1.25 & 0 & 0 \end{bmatrix} + q \begin{bmatrix} 0 & 0 & 0 & 0 \\ 0 & 0 & 0 & 0 \\ -.75 & .75 & 0 & 0 \\ .75 & -.75 & 0 & 0 \end{bmatrix} \tag{3.4}$$

where $|q| \leq 1$ is unknown. Note that if $q = 1$ we achieve the maximum value $k = 2$, and

if $q = -1$ we achieve the minimum value $k = .5$. So, in this example, (c.f. eq. (2.3))

$$E = \begin{bmatrix} 0 & 0 & 0 & 0 \\ 0 & 0 & 0 & 0 \\ -.75 & .75 & 0 & 0 \\ .75 & -.75 & 0 & 0 \end{bmatrix} = \begin{bmatrix} 0 \\ 0 \\ .866 \\ -.866 \end{bmatrix} \begin{bmatrix} -.866 & .866 & 0 & 0 \end{bmatrix} \tag{3.5}$$

so that

$$L = \begin{bmatrix} 0 \\ 0 \\ .866 \\ -.866 \end{bmatrix} \qquad N = \begin{bmatrix} -.866 \\ .866 \\ 0 \\ 0 \end{bmatrix} \tag{3.6}$$

We solved equation (2.32) with $\gamma = 1$ and with previous values for ρ and Q_0. The control gains and closed loop poles are listed in Appendix B.1.

The RLQR controller yields the transients shown in figure 3-3. In this instance, the output transient $y(t)$ looks very similar for all values of the spring constant. Comparing figures 3-2 and 3-3, it is apparent that we achieved a certain level of performance robustness with the RLQR design, as compared to the nominal one.

Additionally, there are some other interesting properties of these simulations. We noted that in this system the uncertainty is contained solely in the potential energy of the spring. The RLQR control responded, in all cases, so as to first move the two masses so that the spring was at its equilibrium length, $(x_1 - x_2) \approx 0$, (in which case there is small uncertainty in the stored potential energy), and next the RLQR control moves the two masses together slowly back to the desired equilibrium position. This behavior was quite different than that of the classical LQR mismatched designs when the system moved the masses towards their zero position and then reduced the spring length to equibrium. Thus the RLQR design acted as if it "knew" that the uncertainty was in the spring constant, and it worked to keep the uncertainty in the spring potential energy from adversely affecting the dynamics of the motion. This was accomplished by the two

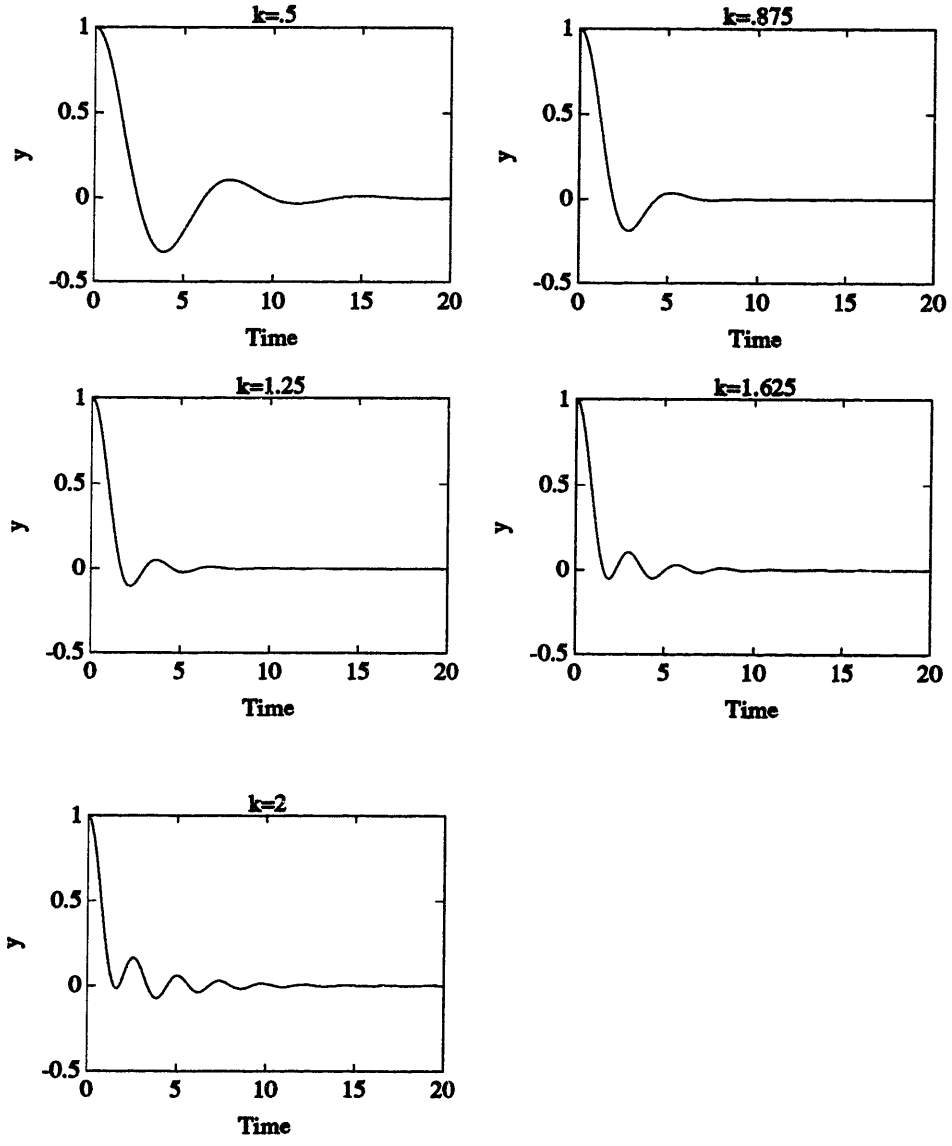

Figure 3-2: Output Response of Mismatched LQR Design. The nominal LQR control was computed for $k = 1.25$. Note the undesirable output oscillations.

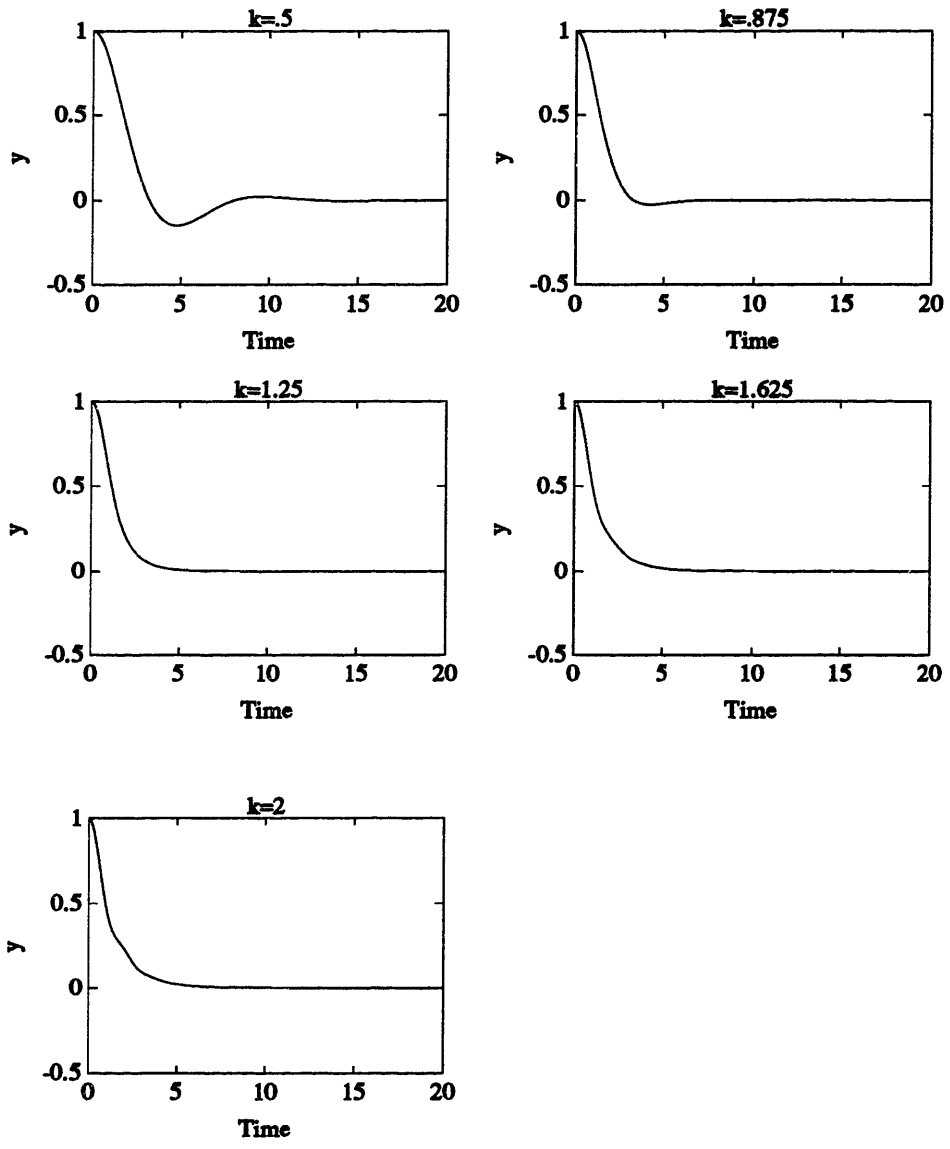

Figure 3-3: Output Response of Robust Design. Note the almost identical output transients especially in the range $0.875 \leq k \leq 2.0$. This we interpret as performance robustness.

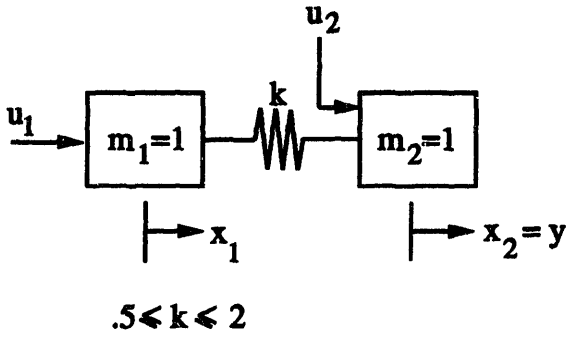

Figure 3-4: The Benchmark Problem with an Additional Control Force

additional terms γNN^T and $\frac{1}{\gamma}PLL^TP$ in the modified Riccati Equation (2.32).

This, and other simulations, suggested to us that the RLQR design may have interesting interpretations from a physical viewpoint, beyond the initial mathematical development which attempted to preserve the robustness properties of standard LQR designs.

3.1.2 The Impact of Additional Control Variables

Since the physical interpretations of the RLQR control was to move m_1 and m_2 to force the uncertain spring to its equilibrium length, it is natural to inquire whether adding another control acting on mass m_2 would further improve the performance robustness since we now have two forces acting on both sides of the spring. See figure 3-4

Using the same values for the design parameters as in section 3.1.1, we simulated both a mismatched LQR design, as shown in figure 3-5, and an RLQR design, shown in figure 3-6. The control gains and closed loop poles are shown in Appendix B.2.

It is clear that the additional control is greatly improving the performance of the system. The settling time is significantly decreased. In the mismatched LQR design, the transients still vary with different values of the spring constant, but not by nearly as much as before. In the RLQR design, the transients are all very similar, even for the case when the spring constant attains its lowest value $k = .5$. Thus we see we have improved transients in both designs.

In the mismatched design, the controller uses the extra available control to reduce

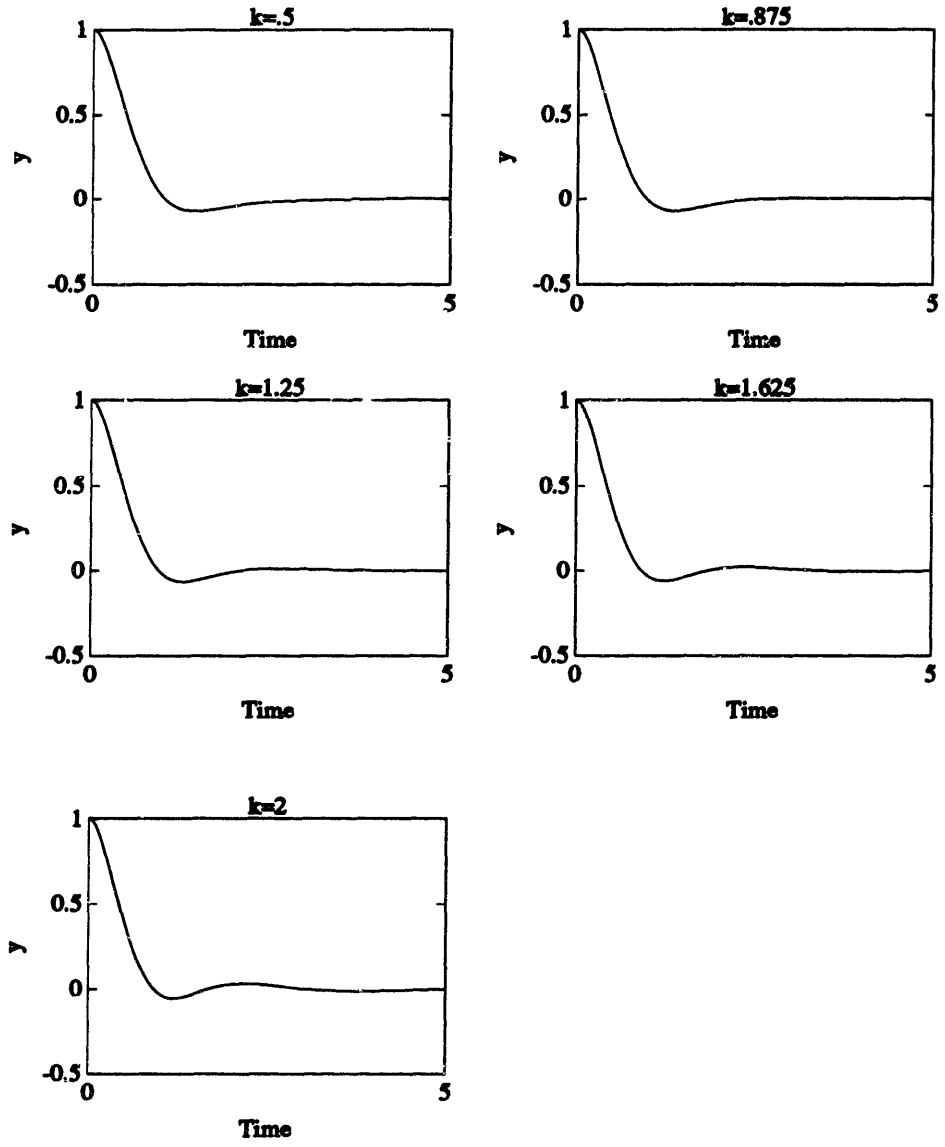

Figure 3-5: Output Response of Mismatched LQR Design with Additional Control (design value $k = 1.25$).

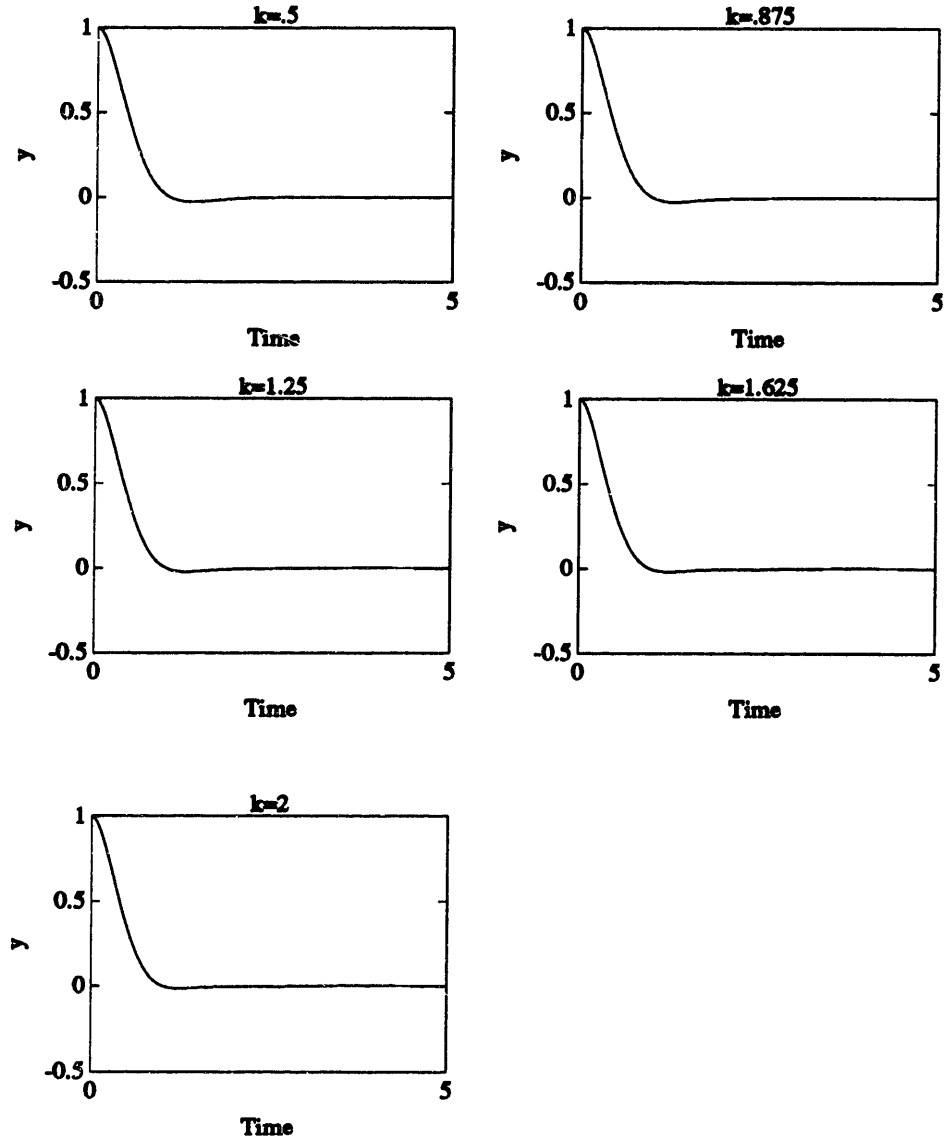

Figure 3-6: Output Response of RLQR Design with Additional Control.

the value of the cost defined by the cost functional. This includes moving the position of the second mass back to equilibrium quicker. The position of the first mass is not directly included in the cost, and thus the controller does not care directly where mass m_1 is, other than in the way it will affect mass m_2.

In the robust design, the extra control lets us get to the zero potential energy state in less time. Thus, for the RLQR design, we are minimizing the effects of uncertain dynamics of the system much quicker. This implies moving the masses so that the spring is at its equilibrium length, thereby eliminating uncertainty in the stored potential energy. Since the controller can now directly influence both ends of the spring, it is easier for it to set the length of the spring to the equilibrium value. Thus we are increasing the performance of the robust design by allowing it to take the uncertainty out of the dynamics in a shorter time period.

We can therefore conclude that the additional control greatly increases our performance. This is not surprising since additional controls give us more degrees of freedom in dealing with the uncertainty.

3.2 Control at the Output

Let us now consider the case when the control directly influences the output, as shown in figure 3-7. The control directly affects the position we wish to control, yet there are uncertain dynamics affecting that position.

The system in this setup can be written as $\dot{x}(t) = Ax(t) + Bu(t)$, with

$$x(t) = \begin{bmatrix} x_1(t) \\ x_2(t) \\ x_3(t) \\ x_4(t) \end{bmatrix} \qquad A = \begin{bmatrix} 0 & 0 & 1 & 0 \\ 0 & 0 & 0 & 1 \\ -k & k & 0 & 0 \\ k & -k & 0 & 0 \end{bmatrix} \qquad B = \begin{bmatrix} 0 \\ 0 \\ 0 \\ 1 \end{bmatrix} \tag{3.7}$$

Note that the A matrix is the same as in section 3.1.1, and so we have chosen the same

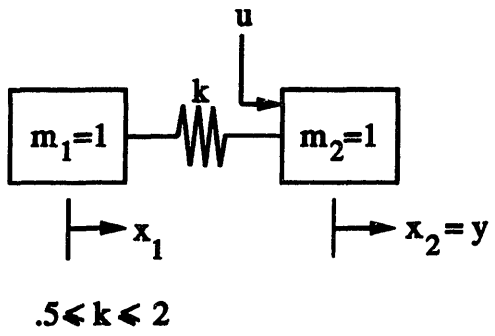

Figure 3-7: System with Control at Output

design parameters as before. The difference is in the B matrix. The resulting gains and closed loop poles are shown in Appendix B.3.

Typical transients are shown in figures 3-8 and 3-9. The potential energy (PE) of the spring is also plotted so that we can directly determine the difference between the two designs. We wish to determine if the controllers will reduce the length of the uncertain spring to equilibrium, and since the controllers directly affect the position of mass m_2, we have chosen the initial condition to be $x_1(0) = 1$. This choice of initial conditions will cause the differences in potential energy between the two designs to be more apparent.

Once again it is clear that the RLQR design handles the uncertain potential energy better than the mismatched design. However, it is also clear the penalty which we pay. The displacement of the output mass is significantly higher in the RLQR design than in the mismatched design. The larger transients are a result of the controller's desire to mitigate the impact of uncertain energy. Thus, mass m_2 must be displaced so the spring is at equilbrium.

3.3 A Two Spring Example

We would like to determine if the energy-based intepretation of the RLQR results will still hold true for more complex systems with more than one uncertain spring. For example, consider the system in figure 3-10, consisting of three unit masses connected

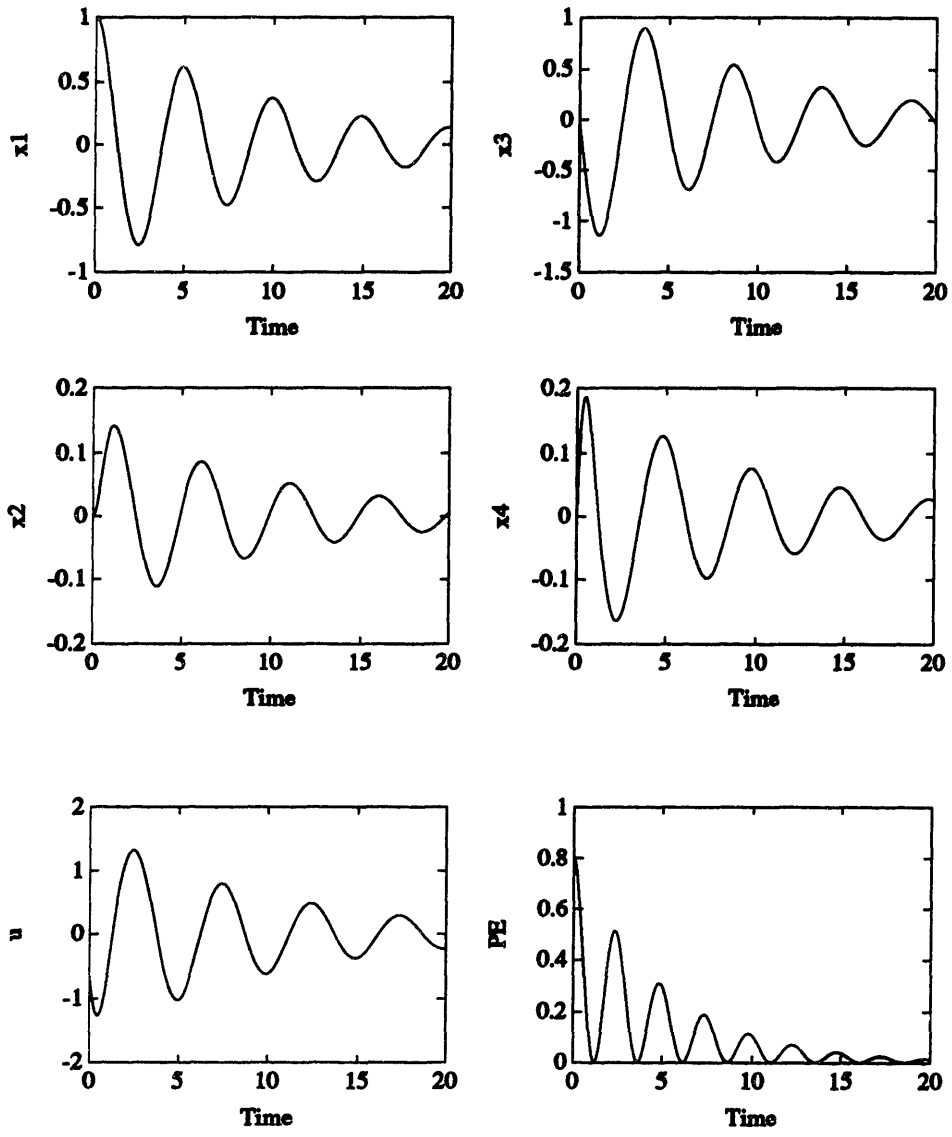

Figure 3-8: Typical Transients of Mismatched LQR Design for System with Control at the Output, with $k = 1.625$, initial state $x(0)$ =[1 0 0 0]. The plot PE indicates the stored potential energy.

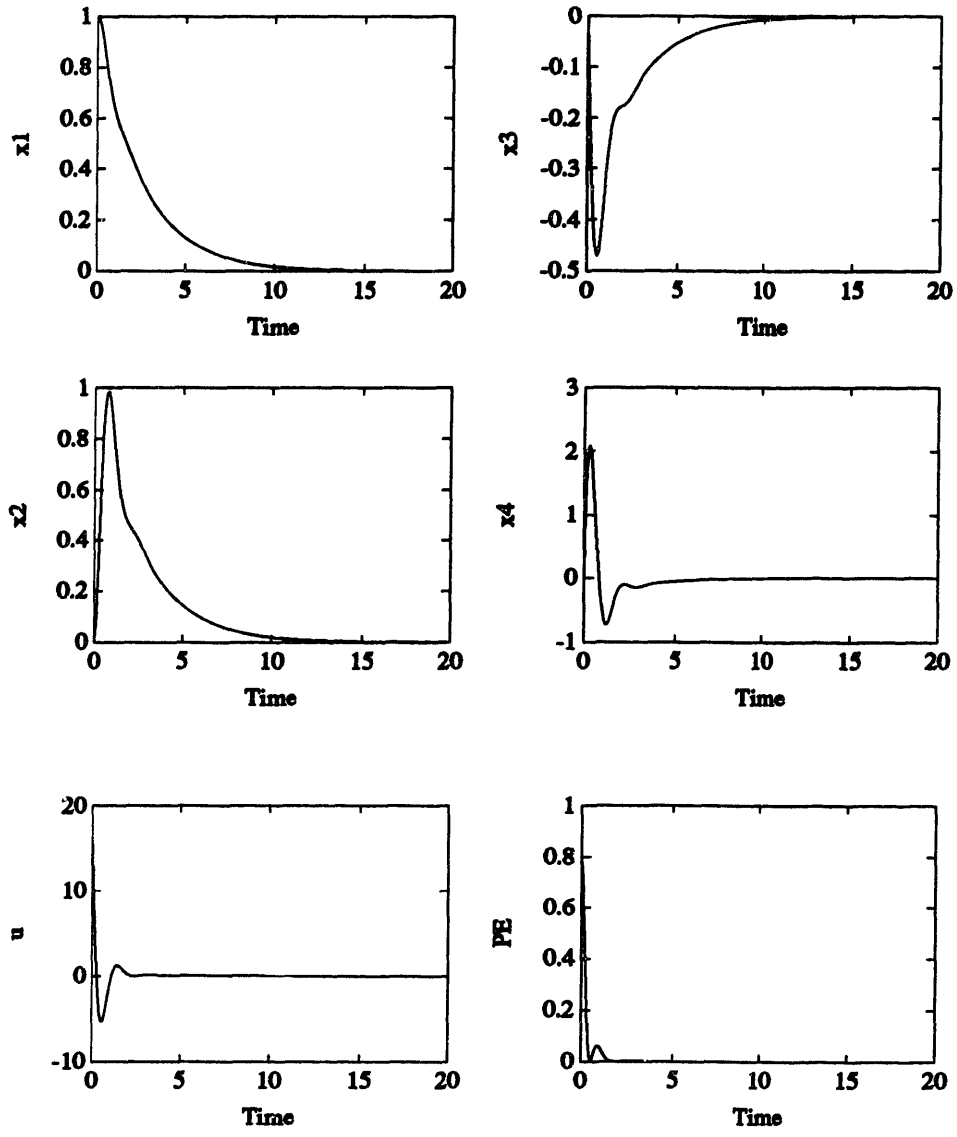

Figure 3-9: Typical Transients of RLQR Design for System with Control at the Output, with $k = 1.625$, initial state $x(0)$ =[1 0 0 0]. The plot PE indicates the stored potential energy.

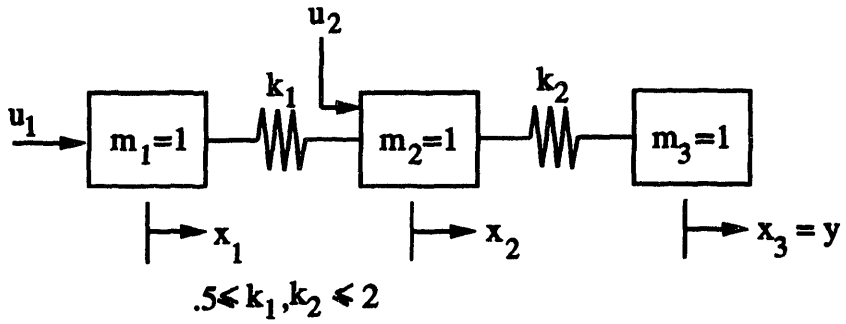

Figure 3-10: Two Spring Example

by two uncertain springs, $k_1, k_2 \in [.5, 2]$. We wish to regulate the position y of mass m_3, using the two controls acting on m_1 and m_2.

We can write our uncertain system as $\dot{x} = Ax + Bu$, with

$$x = \begin{bmatrix} x_1 \\ x_2 \\ x_3 \\ x_4 \\ x_5 \\ x_6 \end{bmatrix} \qquad A = \begin{bmatrix} 0 & 0 & 0 & 1 & 0 & 0 \\ 0 & 0 & 0 & 0 & 1 & 0 \\ 0 & 0 & 0 & 0 & 0 & 1 \\ -k_1 & k_1 & 0 & 0 & 0 & 0 \\ k_1 & -k_1 - k_2 & k_2 & 0 & 0 & 0 \\ 0 & k_2 & -k_2 & 0 & 0 & 0 \end{bmatrix} \qquad B = \begin{bmatrix} 0 & 0 \\ 0 & 0 \\ 0 & 0 \\ 1 & 0 \\ 0 & 1 \\ 0 & 0 \end{bmatrix} \tag{3.8}$$

with x_1 x_2, and x_3 the positions of the masses, and x_4 x_5, and x_6 their respective deriva-

tives. Thus, we can write the uncertain A matrix as

$$A = \begin{bmatrix} 0 & 0 & 0 & 1 & 0 & 0 \\ 0 & 0 & 0 & 0 & 1 & 0 \\ 0 & 0 & 0 & 0 & 0 & 1 \\ -1.25 & 1.25 & 0 & 0 & 0 & 0 \\ 1.25 & -2.5 & 1.25 & 0 & 0 & 0 \\ 0 & 1.25 & -1.25 & 0 & 0 & 0 \end{bmatrix} + q_1 \begin{bmatrix} 0 \\ 0 \\ 0 \\ .866 \\ -.866 \\ 0 \end{bmatrix} \begin{bmatrix} -.866 & .866 & 0 & 0 & 0 & 0 \end{bmatrix}$$

$$+ q_2 \begin{bmatrix} 0 \\ 0 \\ 0 \\ 0 \\ .866 \\ -.866 \end{bmatrix} \begin{bmatrix} 0 & -.866 & .866 & 0 & 0 & 0 \end{bmatrix} \tag{3.9}$$

where q_1 determines the value of k_1, and q_2 determines the value of k_2. Thus, we see our L and N matrices are

$$L = \begin{bmatrix} 0 & 0 \\ 0 & 0 \\ 0 & 0 \\ .866 & 0 \\ -.866 & .866 \\ 0 & -.866 \end{bmatrix} \qquad N = \begin{bmatrix} -.866 & 0 \\ .866 & -.866 \\ 0 & .866 \\ 0 & 0 \\ 0 & 0 \\ 0 & 0 \end{bmatrix} \tag{3.10}$$

For purposes of design, we will pick

$$\gamma = 1 \qquad \rho = .01 \qquad Q_0 = \begin{bmatrix} 0 & 0 & 0 & 0 & 0 & 0 \\ 0 & 0 & 0 & 0 & 0 & 0 \\ 0 & 0 & 1 & 0 & 0 & 0 \\ 0 & 0 & 0 & 0 & 0 & 0 \\ 0 & 0 & 0 & 0 & 0 & 0 \\ 0 & 0 & 0 & 0 & 0 & 0 \end{bmatrix} \tag{3.11}$$

The selection of Q_0 implies the nominal goal of regulating the position x_3 of mass m_3. The resulting control gains and closed loop poles are shown in Appendix B.4.

Typical output transients are shown in figure 3-11, where the left column shows the RLQR design for different values of the two spring constants, and the right column shows the corresponding mismatched LQR design for $k_1 = k_2 = 1.25$. The first plot is the "nominal" system output. Thus, the LQR design is optimal in this plot with respect to the standard cost functional.

We once again see that the transient varies significantly as the values of the spring constants change in the mismatched LQR design. Conversely, the RLQR design produces similar transients for all values of the spring stiffnesses. Additionally, the RLQR design still has the same property of seeming to "know" that the uncertainty lies in the potential energy of the springs, and works to keep the springs at equilibrium length. It appears as though the energy interpretation is still valid.

So that the reader can examine the transients of all the state variables, typical transients are shown for the mismatched LQR design (figure 3-12) and the RLQR design (figure 3-13).

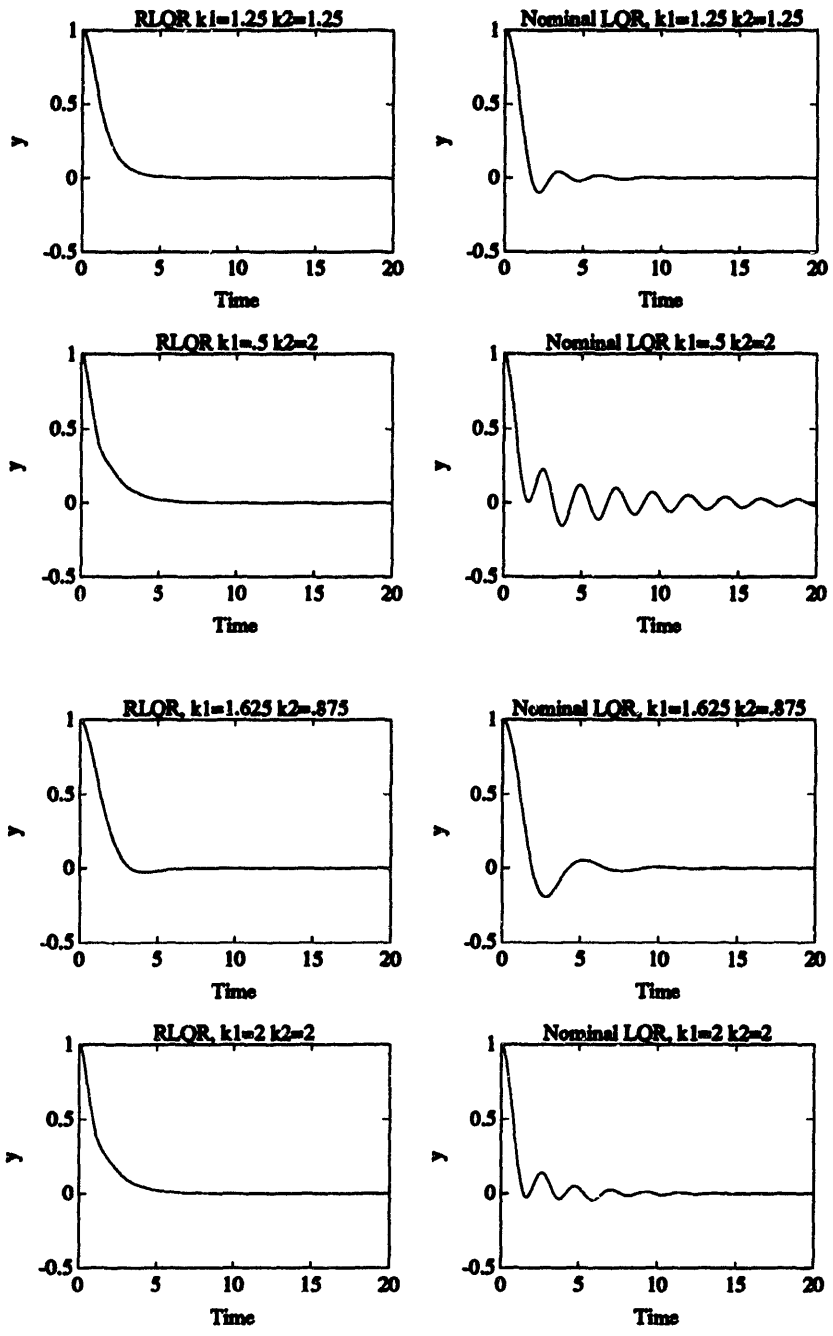

Figure 3-11: Output Response for Two Spring Example. The left column contains RLQR output responses, while the right column denotes mismatched LQR transients (designed with $k_1 = k_2 = 1.25$). The performance robustness of RLQR designs is self-evident.

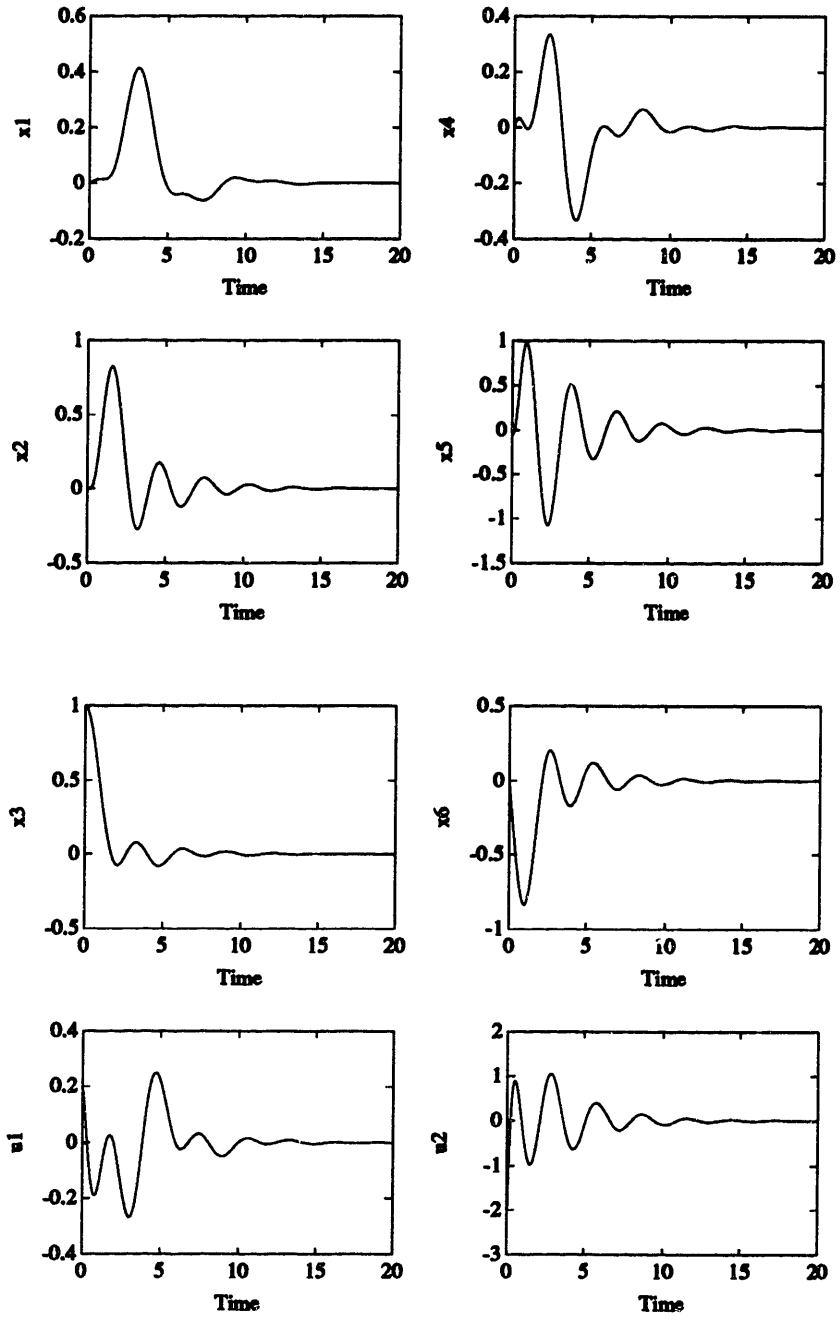

Figure 3-12: Typical Transients of Mismatched LQR Design for Two Spring Example, with $k_1 = .5$, $k_2 = 1.25$.

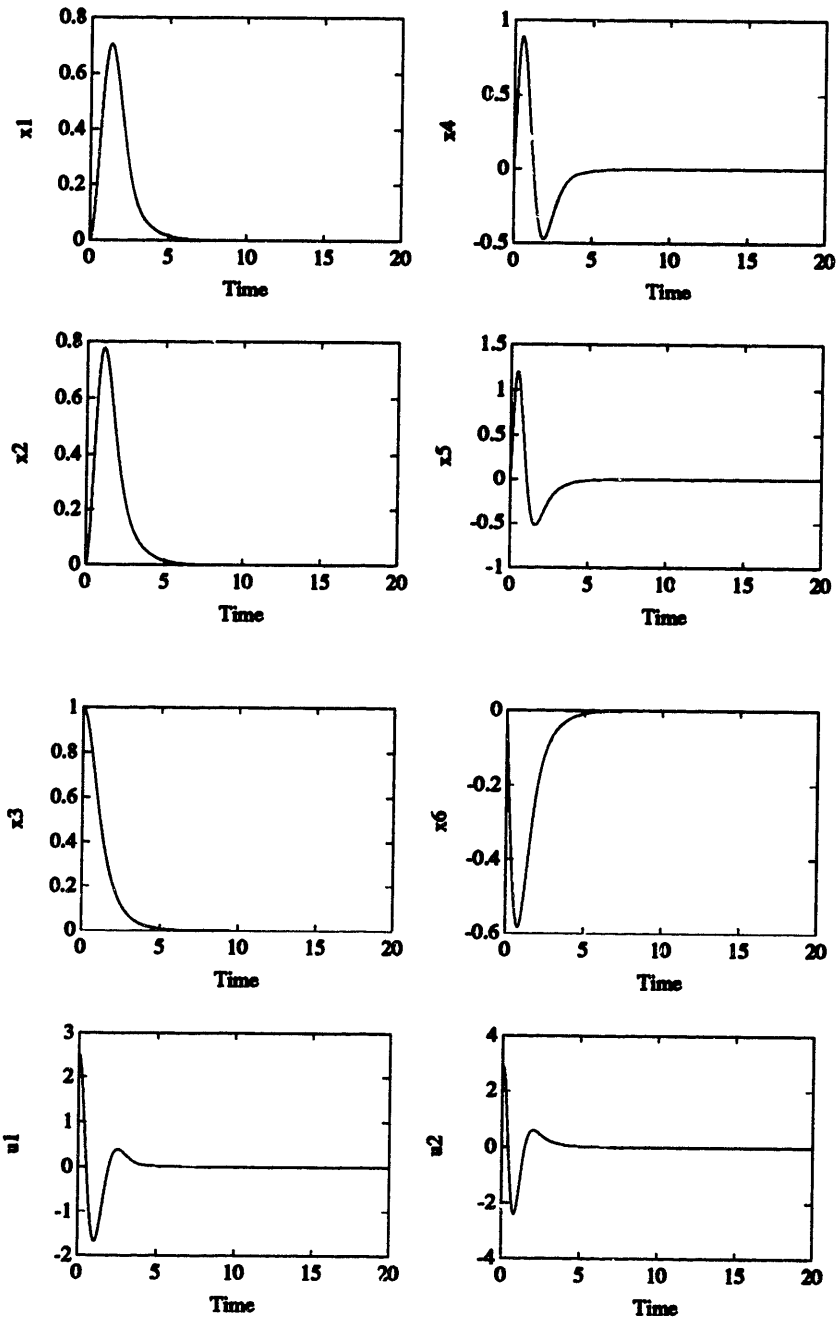

Figure 3-13: Typical Transients of RLQR Design for Two Spring Example, with $k_1 = .5$, $k_2 = 1.25$.

3.4 Partially Known System

If the energy interpretation is valid, the RLQR control should only worry about minimizing the length of uncertain springs. Suppose we let the spring k_2 be known in figure 3-10. We would like to observe how the controllers will behave in this "partially known" system.

We designed both controllers with $k_2 = 1.25$, while as before, $k_1 \in [.5, 2]$. So our A matrix becomes

$$
\begin{aligned}
A &= \begin{bmatrix} 0 & 0 & 0 & 1 & 0 & 0 \\ 0 & 0 & 0 & 0 & 1 & 0 \\ 0 & 0 & 0 & 0 & 0 & 1 \\ -k_1 & k_1 & 0 & 0 & 0 & 0 \\ k_1 & -k_1 - 1.25 & 1.25 & 0 & 0 & 0 \\ 0 & 1.25 & -1.25 & 0 & 0 & 0 \end{bmatrix} \\
&= \begin{bmatrix} 0 & 0 & 0 & 1 & 0 & 0 \\ 0 & 0 & 0 & 0 & 1 & 0 \\ 0 & 0 & 0 & 0 & 0 & 1 \\ -1.25 & 1.25 & 0 & 0 & 0 & 0 \\ 1.25 & -2.5 & 1.25 & 0 & 0 & 0 \\ 0 & 1.25 & -1.25 & 0 & 0 & 0 \end{bmatrix} + q \begin{bmatrix} 0 \\ 0 \\ 0 \\ .866 \\ -.866 \\ 0 \end{bmatrix} \begin{bmatrix} -.866 & .866 & 0 & 0 & 0 & 0 \end{bmatrix}
\end{aligned}
\tag{3.12}
$$

so in this case

$$L = \begin{bmatrix} 0 \\ 0 \\ 0 \\ .866 \\ -.866 \\ 0 \end{bmatrix} \qquad N = \begin{bmatrix} -.866 \\ .866 \\ 0 \\ 0 \\ 0 \\ 0 \end{bmatrix} \tag{3.13}$$

and we once again choose

$$\gamma = 1 \qquad \rho = .01 \qquad Q_0 = \begin{bmatrix} 0 & 0 & 0 & 0 & 0 & 0 \\ 0 & 0 & 0 & 0 & 0 & 0 \\ 0 & 0 & 1 & 0 & 0 & 0 \\ 0 & 0 & 0 & 0 & 0 & 0 \\ 0 & 0 & 0 & 0 & 0 & 0 \\ 0 & 0 & 0 & 0 & 0 & 0 \end{bmatrix} \tag{3.14}$$

The resulting control gains and closed loop poles are shown in Appendix B.5.

Typical transients for this system are shown in figures 3-14 and 3-15 for $k_1 = .5$. Note that since the LQR design was mismatched, the resulting transients contain significant ocsillations. However, the RLQR design once again successfully regulates the output for all values of k_1.

Comparing the transients in figure 3-15 with the previous example in figure 3-13, we see that the RLQR control indeed only reduces the length of the unknown spring. Once again, because of the additional terms in the modified Riccati equation (2.32), the controller "knows" where the uncertainty lies, and mitigates the effect of the uncertain dynamics from the response of the system.

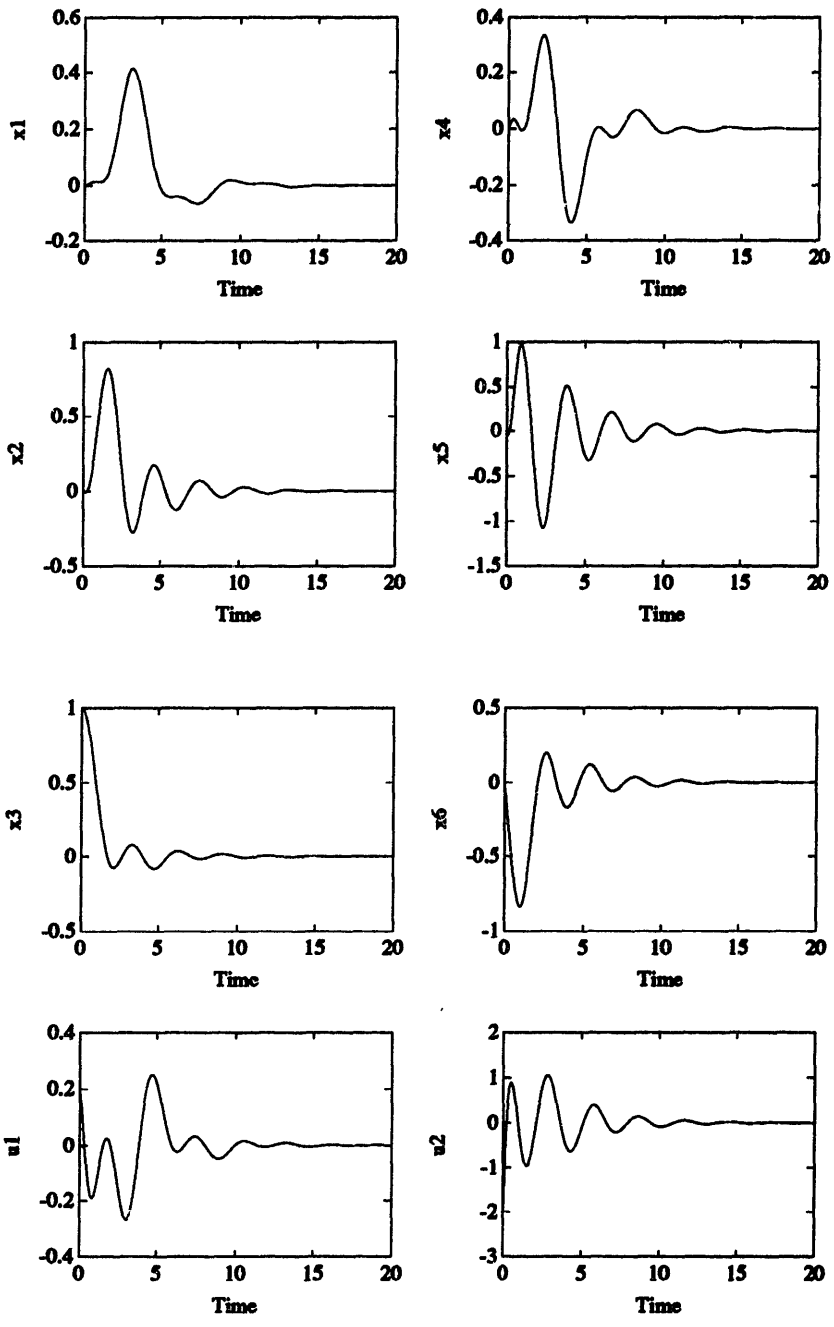

Figure 3-14: Typical Transients of Mismatched LQR Design for Partially Known System, with $k_1 = .5$.

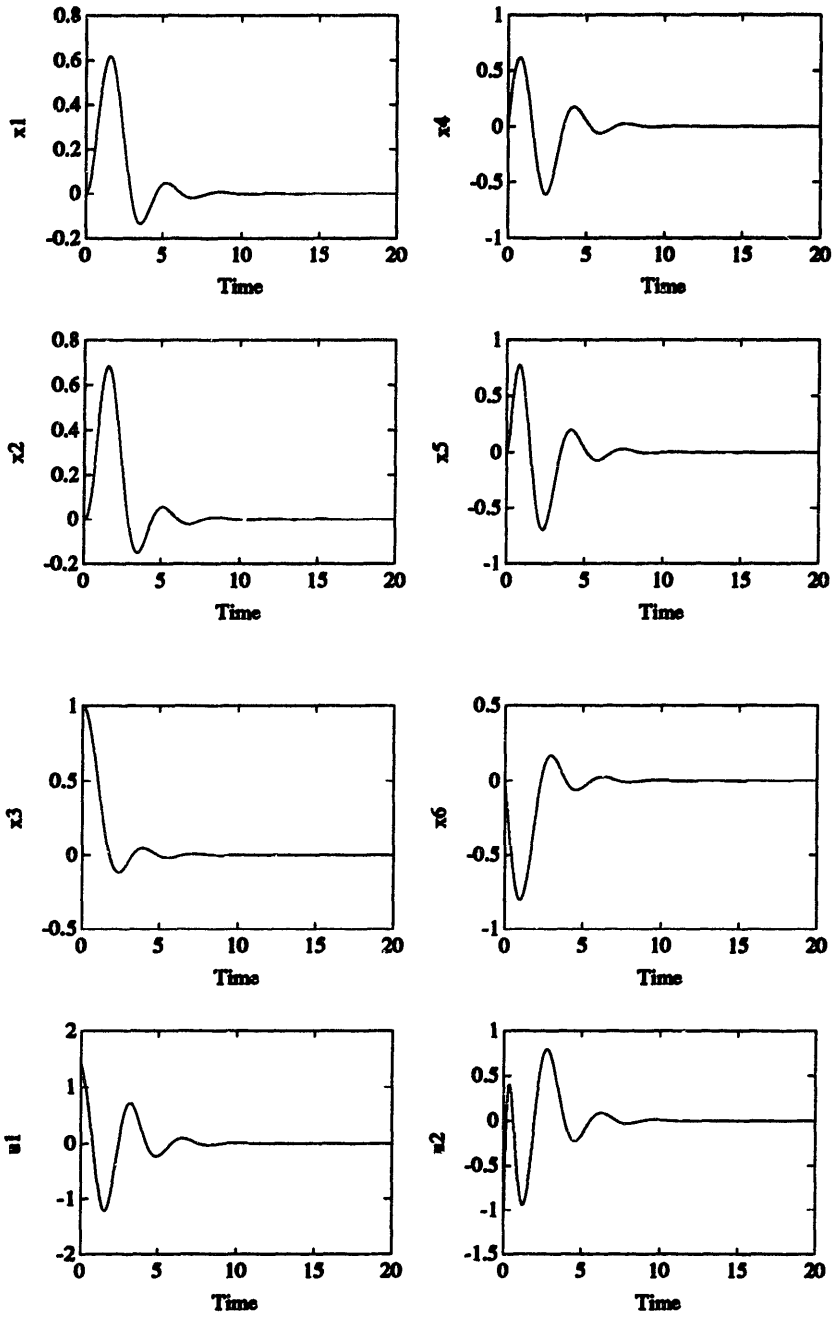

Figure 3-15: Typical Transients of RLQR Design for Partially Known System, with $k_i = .5$

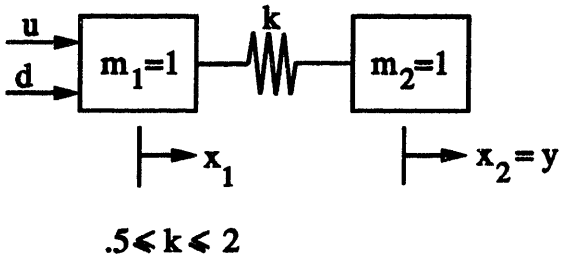

Figure 3-16: The Benchmark Problem with Disturbance at Input

3.5 Disturbances

From the preceding transient simulations, in response to initial conditions, it is obvious that we have gained a certain level of performance robustness in the RLQR design. However, engineering is a set of tradeoffs, and we must ask what they are.

Two obvious candidates are the ability to reject disturbances, and stability-robustness to unstructured uncertainty (e.g. unmodelled dynamics). Given the performance robustness of RLQR in the initial state transients, we should suspect performance robustness in disturbance rejection. This is also to be suspected due to the higher gains associated with the RLQR designs, noted in Appendix B. In this section, we discuss some simulations carried out to test disturbance rejection. We defer discusion of unstructured uncertainty to Chapter 4, when we talk about various properties of the RLQR design.

We now consider a version of the benchmark problem shown in figure 3-16. In addition to our control u, we also have a disturbance d force acting on m_1. Since the uncertain system is the same as in section 3.1.1, we have chosen the same design parameters for both the mismatched LQR design, and the RLQR design. The simulations begin with the system at rest. The control must try to attenuate the disturbance.

As a first disturbance, let us consider simulated white noise. The output transients for the mismatched LQR design are shown in figure 3-17, and for the RLQR design in figure 3-18. We can see that both systems successfully attenuate the disturbance for all values of the spring stiffness. But we see the RLQR design is superior than the mismatched

design, even for the spring stiffness for which the LQR was designed.

Let us try another disturbance which is not broadband. We will apply a pulse function with a period of approximately 9 seconds. This will provide us with a fundamental frequency of .7 rad/sec, which is below the first mode of the mass-spring system, but will have harmonics in the frequency of the first mode. Output transients are shown in figure 3-19 for the mismatched LQR and in figure 3-20 for the RLQR. The RLQR disturbance rejection performance is two to three times better than that of the mismatched LQR design. Both controllers attenuate the disturbance, though the output of the very loose spring ($k = .5$) does appear to be growing in the mismatched LQR design.

Based on these observations, we might conjecture that the RLQR design always has better disturbance rejection than a mismatched LQR design. Indeed, this is so, and it is one of the properties discussed in an analytical framework in Chapter 4.

3.6 Summary

In this chapter we presented and interpreted several simulations. By comparing the behavior of the RLQR controller to a standard LQR design, we have discovered some intriguing properties. The RLQR design appears to minimize the uncertain stored potential energy in the springs, and thus produces very similar outputs for different values of the uncertain stiffness parameters. The RLQR also seems able to reject disturbances better than a mismatched LQR controller.

Comparing the RLQR design to the mismatched LQR design, we see that the RLQR design provides higher gains. In doing so, it is effectively adding more damping to the system, moving the closed-loop poles farther away from the $j\omega$ axis. It also moved the poles farther away from the uncertain open-loop poles of the system.

In the next chapter, we will examine some of the properties of the RLQR controller in greater detail. We will provide some analytical interpretations and explanations of why the RLQR design added performance robustness while preserving stability, and

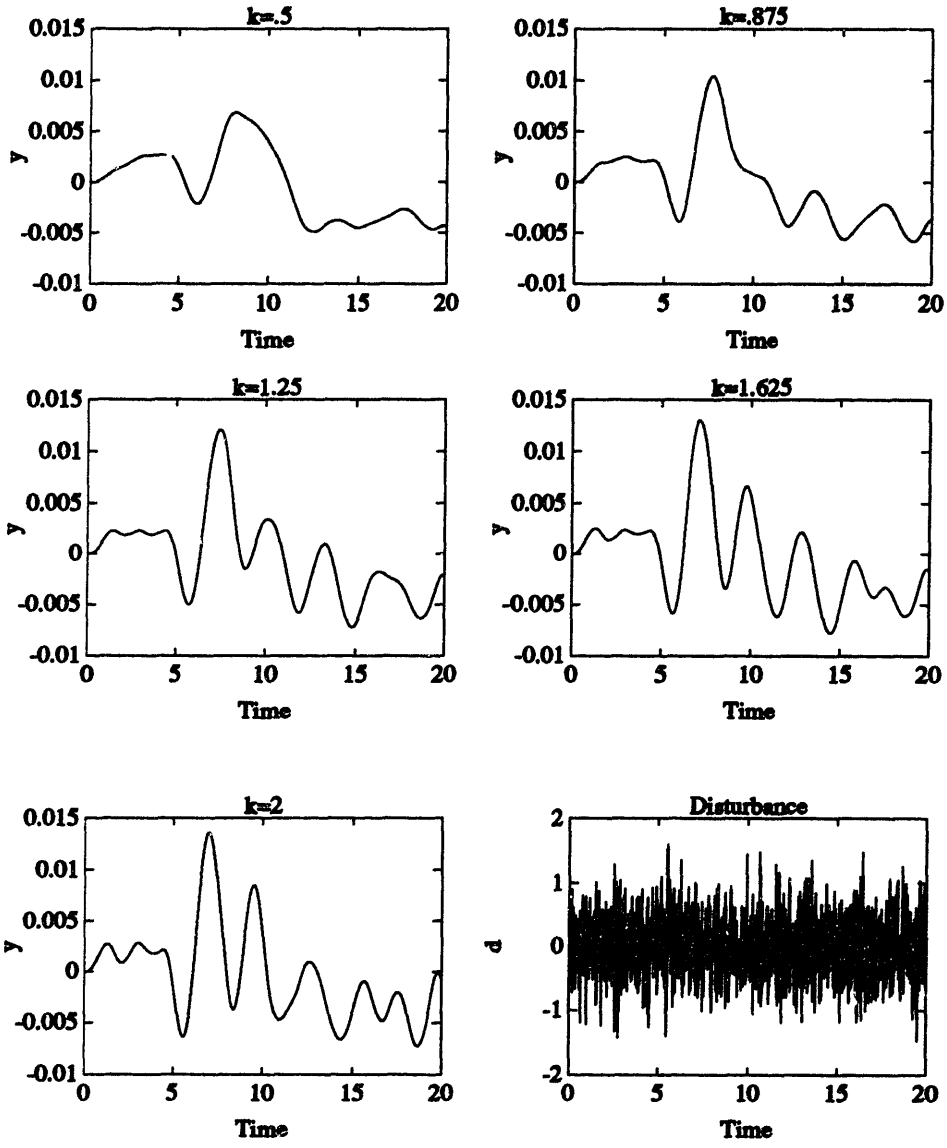

Figure 3-17: Output Response of Mismatched LQR Design with White Noise.

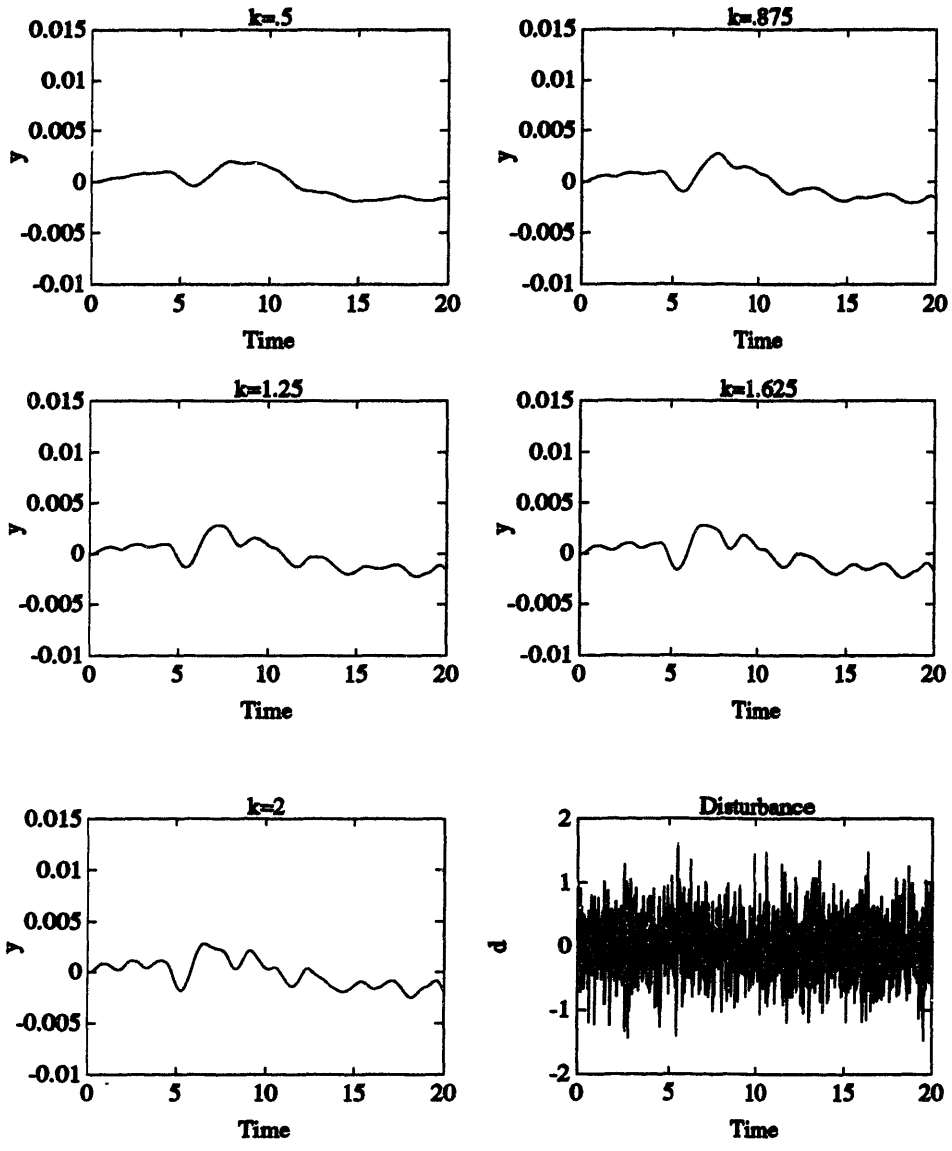

Figure 3-18: Output Response of RLQR Design with White Noise.

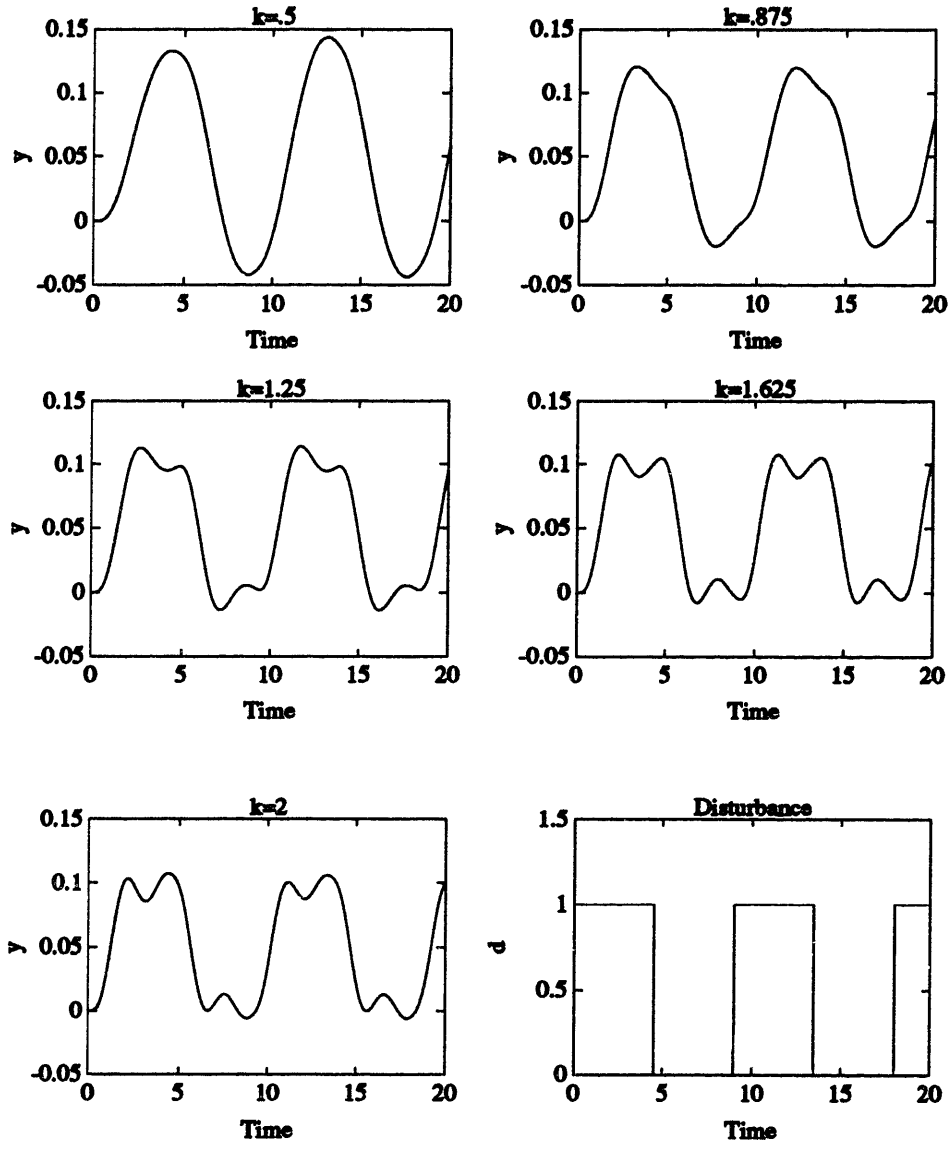

Figure 3-19: Output Response of Mismatched LQR Design with Pulse Disturbance.

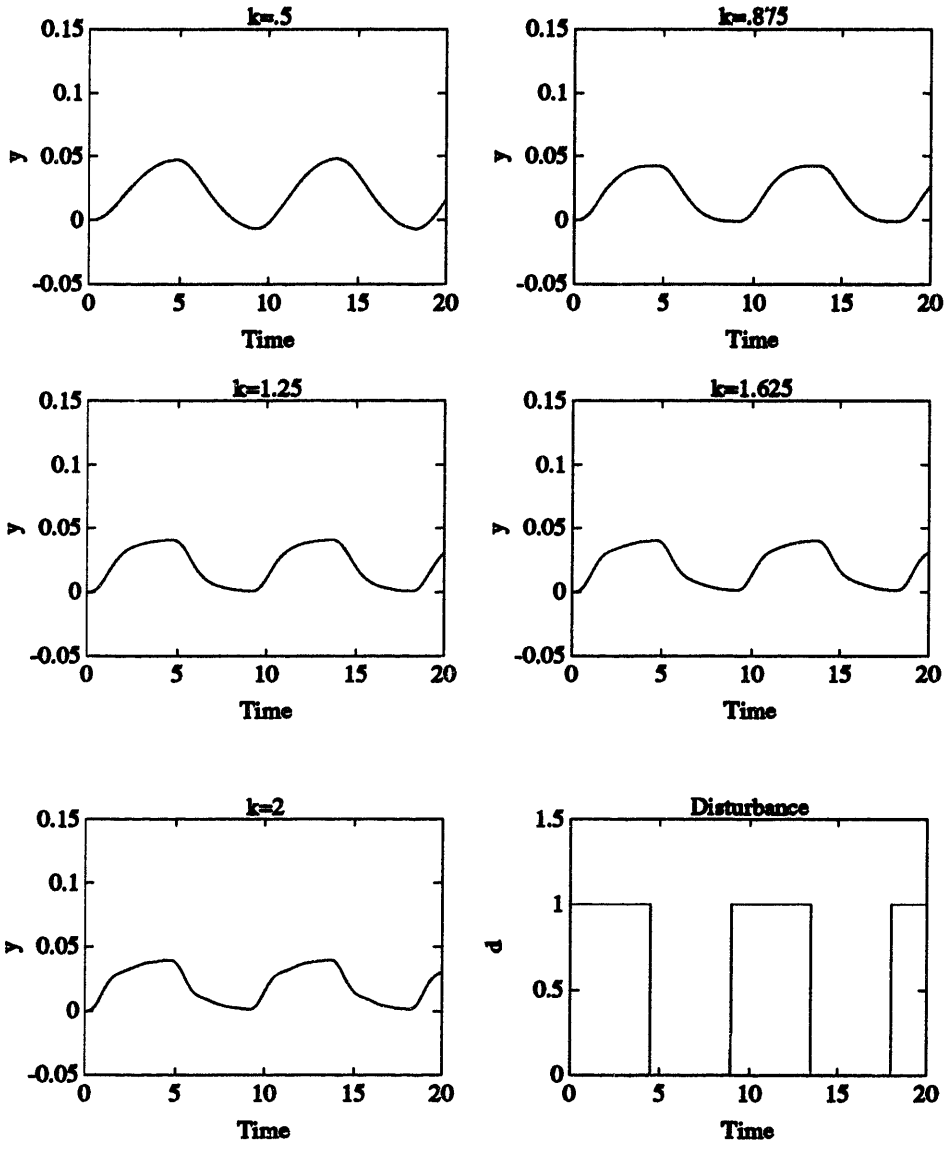

Figure 3-20: Output Response of RLQR Design with Pulse Disturbance.

why it was able to minimize the impact of the uncertain energy. We will also examine the bandwidth of the RLQR design, and its implications in robustness to unstructured uncertainty. We will generalize the results to general systems composed of uncertain springs and also uncertain dampers.

Chapter 4

Properties of RLQR

In this chapter, we will show various properties of the RLQR design. These properties will explain the interesting behavior of the controller in the simulations, and summarize the characteristics of the robust controller. First we will show how we can interpret the RLQR controller in terms of LQR designs. Then we will extend the interpretations to more general systems. This will lead to an understanding of how the parameter γ affects performance. We will then show that have better performance robustness than mismatched LQR designs. Finally, we will demonstrate that the RLQR design is conservative with respect to stability robustness.

4.1 Interpretations

4.1.1 Equivalent LQR Problem

First, we will look at the RLQR design as equivalent to an LQR design. This will explain why we are guaranteed the same robustness as in LQR designs - because it is an LQR design itself.

If we find a solution $P = P^T > 0$ in the Robust Riccati equation (2.32), we could

define a matrix Q by

$$Q \triangleq -PA_0 - A_0^T P + \frac{1}{\rho} PBB^T P = Q_0 + \gamma NN^T + \frac{1}{\gamma} PLL^T P \tag{4.1}$$

Then the RLQR controller is the optimal controller when we are minimizing the cost functional

$$J = \int_0^\infty (x^T(t)Qx(t) + \rho u^T(t)u(t))dt \tag{4.2}$$

Thus the RLQR can be interpreted as an LQR design, with a suitably modified state weighting matrix Q. As shown in the next section, it is the way in which this Q matrix is defined which makes the design robust to parametric uncertainty.

4.1.2 Equivalent Cost Functional

Substituting $Q = Q_0 + \gamma NN^T + \frac{1}{\gamma} PLL^T P$ into the cost functional (4.2), we can write

$$J = \int_0^\infty (x^T(t)Q_0x(t) + x^T(t)\gamma NN^T x(t) + x^T(t)\frac{1}{\gamma} PLL^T Px(t) + \rho u^T(t)u(t))dt \tag{4.3}$$

Let us interpret each term in this cost functional.

The quadratic term $x^T(t)Q_0x(t)$ is the state weighting, and represents the performance penalty we would choose in the nominal case of no uncertainty, as discussed in Chapter 2.

The quadratic term $\gamma x^T(t)NN^T x(t)$ is equal to $1.5\gamma(x_1 - x_2)^2$ in the benchmark problem in section 3.1.1, which is proportional to the uncertain stored potential energy in the spring in that example. We observed in the simulations in section 3.1.1 that the RLQR controller reduced the uncertain potential energy; this is because we were designing an optimal controller which minimized a cost functional containing this energy. In section 4.2, we will show that in general the RLQR minimizes the potential energy of uncertain stiffness elements, and show a similar result for uncertain dampers. This will explain our observations of the uncertain energy reduction in all of the simulations.

The quadratic term $\frac{1}{\gamma} x^T(t)PLL^T Px(t)$ in equation (4.3) is equivalent to an $\mathcal{H}_\infty$ term.

In fact, we could replace this term in the cost functional with a disturbance term $-\gamma d(t)^T d(t)$, which represents a disturbance coming into the system in the direction of the "L" matrix:

$$\dot{x}(t) = A_0 x(t) + Bu(t) + Ld(t) \tag{4.4}$$

Thus, through this term $\frac{1}{\gamma} x^T(t) P L L^T P x(t)$ we are finding the disturbance which maximizes the cost functional, or the worst possible disturbance coming through the L matrix. Of course, this "equivalent" disturbance arises from the mismatched dynamics. For more on $\mathcal{H}_\infty$ controllers in this state-space setting, see [12]. In section 4.5.3, we will compare this $\mathcal{H}_\infty$ disturbance to the actual errors in the system.

The quadratic term $\rho u^T(t) u(t)$ is the control weighting term, which is necessary to prevent infinite control magnitudes. The numerical value of $\rho > 0$ is important in determining the bandwidth of the system.

Thus we can interpret our results as adding guaranteed stability robustness to structured uncertainty and robustness guarantees by adding terms to the nominal LQR cost functional. These terms have the effect of minimizing the impact of the uncertain potential energy of the spring, and hedge against a worst-possible disturbance acting in the directions defined by the uncertain parameters. The relative importance of these terms in the cost functional is determined by the trade-off scalar γ. This issue will be explored further in section 4.3.

4.2 Generalizations

4.2.1 Uncertain Springs

We want to extend the RLQR results for more general systems. Specifically, we wish to intepret the $\gamma x^T(t) N N^T x(t)$ term in the equivalent cost functional (4.3) and determine if the potential energy interpretation is valid. As an example, we assume that we deal

with a structural dynamic system, which can be written as

$$M\ddot{\nu}(t) + D\dot{\nu}(t) + (K + \tilde{K})\nu(t) = f(t) \tag{4.5}$$

where $\nu(t)$ is a generalized position vector, $f(t)$ is a force vector, $M = M^T > 0$ is a mass matrix, $D = D^T \geq 0$ is a damping matrix, $K = K^T \geq 0$ is a stiffness matrix consisting of elements whose stiffness values are known, and $\tilde{K} = \tilde{K}^T \geq 0$ is a stiffness matrix consisting of uncertain elements. We can rewrite the system (4.5) as

$$\begin{bmatrix} \dot{\nu}(t) \\ \ddot{\nu}(t) \end{bmatrix} = \left[\begin{array}{c|c} 0 & I \\ \hline -M^{-1}K - M^{-1}\tilde{K} & -M^{-1}D \end{array}\right] \begin{bmatrix} \nu(t) \\ \dot{\nu}(t) \end{bmatrix} + \begin{bmatrix} 0 \\ M^{-1} \end{bmatrix} f(t) \tag{4.6}$$

Note that the system has the nominal matrix

$$\left[\begin{array}{c|c} 0 & I \\ \hline -M^{-1}K & -M^{-1}D \end{array}\right] \tag{4.7}$$

and an uncertain term

$$\left[\begin{array}{c|c} 0 & 0 \\ \hline -M^{-1}\tilde{K} & 0 \end{array}\right] \tag{4.8}$$

Let us assume there are p uncertain stiffness parameters in the system. Then we will write

$$\tilde{K} = \sum_{i=1}^{p} \tilde{r}_i \tilde{K}_i \tag{4.9}$$

where $\tilde{K}_i = \tilde{K}_i^T \geq 0$ is a known matrix which represents the structure of how the i^{th} uncertain stiffness element affects the system, and $\tilde{r}_i > 0$ is a scalar which represents the uncertain value of the unknown stiffness element. Let us assume, as is true in mass-spring-dashpot systems, that each $\tilde{K}_i$ is rank 1.

Given uncertainty intervals for each uncertain stiffness element, we can scale each $\tilde{K}_i$ so as to write

$$\tilde{r}_i = \tilde{r}_{i0} + q_i \qquad |q_i| \leq 1 \tag{4.10}$$

where $\tilde{r}_{i0}$ is the "nominal" value of the i^{th} uncertain element, and is chosen at the midpoint of the interval, and q_i represents the uncertain value.

To make this setup more clear, let us see how the examples of chapter 3 fit into this framework. The benchmark problem of figure 3-1 can be written as $\dot{x}(t) = Ax(t) + Bu(t)$ with values listed in equation (3.1), repeated here:

$$x = \begin{bmatrix} x_1 \\ x_2 \\ x_3 \\ x_4 \end{bmatrix} \qquad A = \begin{bmatrix} 0 & 0 & 1 & 0 \\ 0 & 0 & 0 & 1 \\ -k & k & 0 & 0 \\ k & -k & 0 & 0 \end{bmatrix} \qquad B = \begin{bmatrix} 0 \\ 0 \\ 1 \\ 0 \end{bmatrix} \tag{4.11}$$

This example fits in the general framework with the parameters

$$M = \begin{bmatrix} 1 & 0 \\ 0 & 1 \end{bmatrix} \qquad D = \begin{bmatrix} 0 & 0 \\ 0 & 0 \end{bmatrix} \qquad \nu(t) = \begin{bmatrix} x_1(t) \\ x_2(t) \end{bmatrix} \tag{4.12}$$

$$K = \begin{bmatrix} 0 & 0 \\ 0 & 0 \end{bmatrix} \qquad \tilde{K} = \begin{bmatrix} -k & k \\ k & -k \end{bmatrix} \qquad f(t) = \begin{bmatrix} u(t) \\ 0 \end{bmatrix} \tag{4.13}$$

Since $k \in [.5, 2]$, we can write $\tilde{K} = (\tilde{r}_{10} + q_1)\tilde{K}_1$, with the values

$$\tilde{r}_{10} = 1.25 \qquad \tilde{K}_1 = \begin{bmatrix} -.75 & .75 \\ .75 & -.75 \end{bmatrix} \qquad |q_1| \leq 1 \tag{4.14}$$

Note that $D = 0$ because we assume no damping in figure 3-1, and that $K = 0$ because there are no known stiffness elements.

As a second example, let's look at the two spring example of figure 3-10. We have previously written the system in the form $\dot{x}(t) = Ax(t) + Bu(t)$, with the values listed in

equation (3.8), which are:

$$x = \begin{bmatrix} x_1 \\ x_2 \\ x_3 \\ x_4 \\ x_5 \\ x_6 \end{bmatrix} \qquad A = \begin{bmatrix} 0 & 0 & 0 & 1 & 0 & 0 \\ 0 & 0 & 0 & 0 & 1 & 0 \\ 0 & 0 & 0 & 0 & 0 & 1 \\ -k_1 & k_1 & 0 & 0 & 0 & 0 \\ k_1 & -k_1 - k_2 & k_2 & 0 & 0 & 0 \\ 0 & k_2 & -k_2 & 0 & 0 & 0 \end{bmatrix} \qquad B = \begin{bmatrix} 0 & 0 \\ 0 & 0 \\ 0 & 0 \\ 1 & 0 \\ 0 & 1 \\ 0 & 0 \end{bmatrix} \tag{4.15}$$

In the general framework, our parameters are

$$M = \begin{bmatrix} 1 & 0 & 0 \\ 0 & 1 & 0 \\ 0 & 0 & 1 \end{bmatrix} \qquad D = \begin{bmatrix} 0 & 0 & 0 \\ 0 & 0 & 0 \\ 0 & 0 & 0 \end{bmatrix} \qquad \nu(t) = \begin{bmatrix} x_1(t) \\ x_2(t) \\ x_3(t) \end{bmatrix} \tag{4.16}$$

$$K = \begin{bmatrix} 0 & 0 & 0 \\ 0 & 0 & 0 \\ 0 & 0 & 0 \end{bmatrix} \qquad \tilde{K} = \begin{bmatrix} -k_1 & k_1 & 0 \\ k_1 & -k_1 - k_2 & k_2 \\ 0 & k_2 & -k_2 \end{bmatrix} \qquad f(t) = \begin{bmatrix} u_1(t) \\ u_2(t) \\ 0 \end{bmatrix} \tag{4.17}$$

This time there are two uncertain parameters, $k_1, k_2 \in [.5, 2]$, so we can seperate $\tilde{K}$ as

$$\tilde{K} = (\tilde{r}_{10} + q_1)\tilde{K}_1 + (\tilde{r}_{20} + q_2)\tilde{K}_2 \tag{4.18}$$

$$\tilde{r}_{10} = 1.25 \qquad \tilde{r}_{20} = 1.25 \qquad \tilde{K}_1 = \begin{bmatrix} -.75 & .75 & 0 \\ .75 & -.75 & 0 \\ 0 & 0 & 0 \end{bmatrix} \qquad \tilde{K}_2 = \begin{bmatrix} 0 & 0 & 0 \\ 0 & -.75 & .75 \\ 0 & .75 & -.75 \end{bmatrix} \tag{4.19}$$

The potential energy contained in the general setting (4.5) is equal to

$$\frac{1}{2}\nu^T(t)(K + \tilde{K})\nu(t) \tag{4.20}$$

and we can therefore see that the uncertain potential energy in the system is

$$\frac{1}{2}\nu^T(t)\tilde{K}\nu(t) = \frac{1}{2}\sum_{i=1}^{p}(\tilde{r}_{i0} + q_i)\nu^T(t)\tilde{K}_i\nu(t) \tag{4.21}$$

Hence the potential energy in the i^{th} uncertain stiffness element is

$$\frac{1}{2}(\tilde{r}_{i0} + q_i)\nu^T(t)\tilde{K}_i\nu(t) \tag{4.22}$$

To understand the potential energy setup, we see that the potential energy in the second example of the two spring system of figure 3-10 is

$$\frac{1}{2}\nu^T(t)(K + \tilde{K})\nu(t) = \frac{1}{2}\nu^T(t)\tilde{K}\nu(t) \tag{4.23}$$

$$= \frac{1}{2}(\tilde{r}_{10} + q_1)\nu^T(t)\tilde{K}_1\nu(t) + \frac{1}{2}(\tilde{r}_{20} + q_2)\nu^T(t)\tilde{K}_2\nu(t) \tag{4.24}$$

$$= \frac{1}{2}k_1(x_1(t) - x_2(t))^2 + \frac{1}{2}k_2(x_2(t) - x_3(t))^2 \tag{4.25}$$

We can see the potential energy in the first uncertain spring is $\frac{1}{2}(\tilde{r}_{10} + q_1)\nu^T(t)\tilde{K}_1\nu(t)$, and the potential energy in the second uncertain spring is $\frac{1}{2}(\tilde{r}_{20} + q_2)\nu^T(t)\tilde{K}_2\nu(t)$.

Returning to the general framework, since each $\tilde{K}_i$ is symmetric, positive-semidefinite, and rank 1, we can write

$$\tilde{K}_i = \eta_i\eta_i^T \tag{4.26}$$

where η_i is a vector of appropriate length. However, there are other ways to factor $\tilde{K}_i$, and to represent this in a general form, we will write

$$\tilde{K}_i = (\frac{1}{\gamma_i}\eta_i)(\gamma_i\eta_i^T) \tag{4.27}$$

where γ_i is a scalar scaling factor which represents how we factored the matrix $\tilde{K}_i$. We

can now write the total uncertainty in the RLQR setup of equation (2.2) as

$$\sum_{i=1}^{p} q_i E_i = \sum_{i=1}^{p} \left[\begin{array}{c|c} 0 & 0 \\ \hline -M^{-1}q_i\tilde{K}_i & 0 \end{array}\right] = \sum_{i=1}^{p} q_i \left[\begin{array}{c} 0 \\ -\frac{1}{\gamma_i}M^{-1}\eta_i \end{array}\right] \left[\begin{array}{cc} \gamma_i\eta_i^T & 0 \end{array}\right] \tag{4.28}$$

Note that the midpoint matrix is grouped with the nominal matrix in the RLQR framework, and thus the term $\tilde{r}_{i0}\tilde{K}$ is not in the uncertainty matrix. Also, q_i in the RLQR framework is exactly the same q_i as in equation (4.10), and explains our choice of notation.

We are finally in position to look at the $x^T(t)NN^Tx(t)$ term in the equivalent cost functional (4.3). From equation (4.28), we see our N matrix is

$$N = \left[\begin{array}{cccc} \left[\begin{array}{c} \gamma_1\eta_1 \\ 0 \end{array}\right] & \left[\begin{array}{c} \gamma_2\eta_2 \\ 0 \end{array}\right] & \left[\begin{array}{c} \gamma_3\eta_3 \\ 0 \end{array}\right] & \cdots \end{array}\right] \tag{4.29}$$

so that

$$x^T(t)NN^Tx(t) = \nu^T(t)\left[\begin{array}{cccc} \gamma_1\eta_1 & \gamma_2\eta_2 & \gamma_3\eta_3 & \cdots \end{array}\right] \left[\begin{array}{c} \gamma_1\eta_1^T \\ \gamma_2\eta_2^T \\ \gamma_3\eta_3^T \\ \vdots \end{array}\right] \nu(t) \tag{4.30}$$

$$= \sum_{i=1}^{p} \gamma_i^2 \nu^T(t)\eta_i\eta_i^T\nu(t) \tag{4.31}$$

Comparing equations (4.31) and (4.22) we see that x^TNN^Tx in this general setup is proportional to a weighted sum of the energies in each of the uncertain stiffness elements. The weighting depends upon how the matrix for each uncertain parameter was factored.

Thus, we see that for all structural systems of the form (4.5), the RLQR design minimizes a weighted sum of the uncertain potential energies of the uncertain stiffness parameters. We can conclude that the previous interpretation of minimizing uncertain energy is valid in a more general setting.

4.2.2 Uncertain Dampers

We would also like to interpret the term $x^T(t)NN^Tx(t)$ in the case when there is uncertainty in the "D" matrix in the general system form

$$M\ddot{\nu}(t) + (D + \tilde{D})\dot{\nu}(t) + K\nu(t) = f(t) \tag{4.32}$$

where $\nu(t)$ is the generalized position vector, $f(t)$ is the force vector, $M = M^T > 0$ is a mass matrix, $K = K^T \geq 0$ is a stiffness matrix (which in this example is known), $D = D^T \geq 0$ is a damping matrix consisting of elements whose values are known, and $\tilde{D} = \tilde{D}^T \geq 0$ is a damping matrix consisting of uncertain elements.

In this case, the system equation can be written as

$$\begin{bmatrix} \dot{\nu}(t) \\ \ddot{\nu}(t) \end{bmatrix} = \left[\begin{array}{c|c} 0 & I \\ \hline -M^{-1}K & -M^{-1}D - M^{-1}\tilde{D} \end{array}\right] \begin{bmatrix} \nu(t) \\ \dot{\nu}(t) \end{bmatrix} + \begin{bmatrix} 0 \\ M^{-1} \end{bmatrix} f(t) \tag{4.33}$$

with the uncertain term

$$\left[\begin{array}{c|c} 0 & 0 \\ \hline 0 & -M^{-1}\tilde{D} \end{array}\right] \tag{4.34}$$

Following the same steps as before, assuming p uncertain damping elements, we can write the uncertainty as

$$\tilde{D} = \sum_{i=1}^{p} \tilde{r}\tilde{D}_i = \sum_{i=1}^{p} (\tilde{r}_{i0} + q_i)\tilde{D}_i \qquad |q_i| \leq 1 \tag{4.35}$$

where $\tilde{D}_i = \tilde{D}_i^T \geq 0$ is rank 1, $\tilde{r}_{i0}$ is the scalar representing the midpoint of the bounds on the i^{th} uncertain damper, and q_i represents the uncertainty.

Once again, we factor $\tilde{D}_i$ as

$$\tilde{D}_i = (\frac{1}{\gamma_i}\eta_i)(\gamma_i\eta_i^T) \tag{4.36}$$

We write the uncertainty in the RLQR framework of equation (2.2) as

$$\sum_{i=1}^{p} q_i E_i = \sum_{i=1}^{p} \left[\begin{array}{c|c} 0 & 0 \\ \hline 0 & -M^{-1} q_i \tilde{D}_i \end{array}\right] = \sum_{i=1}^{p} q_i \begin{bmatrix} 0 \\ -\frac{1}{\gamma_i} M^{-1} \eta_i \end{bmatrix} \begin{bmatrix} 0 & \gamma_i \eta_i^T \end{bmatrix} \tag{4.37}$$

This time, we see our N matrix is

$$N = \begin{bmatrix} \begin{bmatrix} 0 \\ \gamma_1 \eta_1 \end{bmatrix} & \begin{bmatrix} 0 \\ \gamma_2 \eta_2 \end{bmatrix} & \begin{bmatrix} 0 \\ \gamma_3 \eta_3 \end{bmatrix} & \cdots \end{bmatrix} \tag{4.38}$$

so that

$$x^T(t) N N^T x(t) = \sum_{i=1}^{p} \gamma_i^2 \dot{\nu}^T(t) \eta_i \eta_i^T \dot{\nu}(t) \tag{4.39}$$

To interpret this term, let us consider the energy in the system (4.32)

$$PE = \frac{1}{2} \nu^T(t) K \nu(t) \qquad KE = \frac{1}{2} \dot{\nu}^T(t) M \dot{\nu}(t) \qquad TE = \frac{1}{2} \nu^T(t) K \nu(t) + \frac{1}{2} \dot{\nu}^T(t) M \dot{\nu}(t) \tag{4.40}$$

where PE is potential energy, KE is kinetic energy, and TE is the total energy of the system, the sum of potential and kinetic energies.

The rate of change of total energy in the system is

$$\frac{d}{dt}(TE) = \frac{1}{2}(\ddot{\nu}^T(t) M \dot{\nu}(t) + \dot{\nu}^T(t) M \ddot{\nu}(t) + \dot{\nu}^T(t) K \nu(t) + \nu^T(t) K \dot{\nu}(t)) \tag{4.41}$$

Substituting equation (4.32) into equation (4.41), we obtain

$$\begin{aligned} \frac{d}{dt}(TE) = \frac{1}{2}(&-\dot{\nu}^T(t)(D + \tilde{D})\dot{\nu}(t) - \nu^T(t) K \dot{\nu}(t) + f^T(t)\dot{\nu}(t) - \dot{\nu}^T(t)(D + \tilde{D})\dot{\nu}(t) \\ &- \dot{\nu}^T(t) K \nu(t) + \dot{\nu}^T(t) f(t) + \dot{\nu}^T(t) K \nu(t) + \nu^T(t) K \dot{\nu}(t)) \end{aligned} \tag{4.42}$$

$$= \dot{\nu}^T(t)(-(D + \tilde{D})\dot{\nu}(t) + f(t)) \tag{4.43}$$

The term $\dot{\nu}(t) f(t)$ is the rate of change of energy due to the force vector, and

$\dot{\nu}^T(t)(D + \tilde{D})\dot{\nu}(t)$ is the rate of dissipation of energy due to the damping matrices (the negative sign signifies energy is leaving the system).

So the rate of change of energy (dissipated power) through the i^{th} uncertain damper is

$$\dot{\nu}^T(t)(\tilde{r}_{i0} + q_i)\tilde{D}_i\dot{\nu}(t) = (\tilde{r}_{i0} + q_i)\dot{\nu}^T(t)\eta_i\eta_i^T\dot{\nu}(t) \tag{4.44}$$

Now we can clearly see that

$$x^T(t)NN^Tx(t) = \sum_{i=1}^{p} \gamma_i^2\dot{\nu}^T(t)\eta_i\eta_i^T\dot{\nu}(t) \tag{4.45}$$

is a weighted sum of energy dissipation rates through the uncertain dampers in the system. Once again, the RLQR design is robust to parametric uncertainty by minimizing the effect of the uncertain energy on the system.

Of course when there is uncertainty in both K and D, it is clear that the $x^T(t)NN^Tx(t)$ term represents a weighted sum of uncertain potential energies and uncertain energy dissipation rates. The weights evolve from the choice of the factorization of E_i into l_i and n_i. Thus, we can use this knowledge to intelligently choose the factorization. We put larger relative weights on those uncertain elements whose dynamics degrade our performance to a greater degree. For example, to further reduce the uncertain potential energy of the i^{th} uncertain spring, we would change our factorization from $E_i = l_in_i^T$ to $E_i = (\frac{1}{\gamma_i}l_i)(\gamma_in_i^T)$, with $\gamma_i > 1$.

4.3 The Role of γ

From the equivalent cost functional in section 4.1.2, we can see that the parameter γ can be interpreted as a tradeoff between minimizing unknown uncertain energy and worst case disturbances in the direction of parametric uncertainty. To understand the tradeoffs, let's look at the limiting cases, when γ is very large or very small.

If γ is very large, we are heavily weighting the uncertain energy in the system. Such

a high weighting is sufficient to robustify the design to parametric uncertainty, since the cost of uncertain dynamics is so high. Conversely, if γ is very small we are heavily weighting the worst case disturbance in the direction of the uncertainty. As γ approaches zero[1], we are not allowing any disturbance in this "uncertainty direction," and therefore not allowing the uncertain parameter to influence the response.

So an intermediate value of γ is a tradeoff between penalizing the uncertain energy, and a worst-case equivalent disturbance. Since γ affects the bandwidth of the closed-loop system, an intermediate value is desired (very high or very low γ results in a high bandwidth). It is not surprising to find the bandwidth of the system with the RLQR design higher than that with the mismatched LQR design, since we are desensitising the system to parameter variations. The parameter γ can help tune the bandwidth to an acceptable level. Note that a higher bandwidth implies less robustness to high-frequency unstructured uncertainty [1]. This is one of the prices we pay for robustness to parametric uncertainty. The impact of γ on bandwidth and robustness to unstructured uncertainty will be illustrated in the next section.

4.4 Guaranteed Performance

We observed in the simulations that the RLQR design attenuated disturbances. This should not be surprising: when we guaranteed $\sigma_i[I + G_{LQR}(s)] \geq 1$ is section 2.3.2, we guaranteed the singular values of the sensitivity function are less than unity, i.e. $\sigma_i[I + G_{LQR}(s)]^{-1} \leq 1$, and therefore we have guaranteed performance robustness. This is a property of LQR designs (though note that it is not guaranteed to hold when we design an LQR controller for one system and apply it to another system).

What is more surprising was that the RLQR design seemed to attenuate disturbances better than the mismatched LQR design. We will now prove that we are guaranteed better performance robustness in an RLQR design than a mismatched LQR design.

[1]Note that such a controller will not exist in general, since we are forcing the system to completely eliminate the effect of the disturbances.

First, a preliminary lemma we will need later in the proof:

Lemma 4.1 *Suppose $X \geq Y \geq 0$, with X and Y symmetric. Then $\lambda_{min}(X) \geq \lambda_{min}(Y)$.*

Proof 4.1 *For $Z \geq 0$, Z symmetric, then*

$$\lambda_{min}(Z) = \min_{||x||=1} x^T Z x \tag{4.46}$$

Thus we have

$$\lambda_{min}(X) = \min_{||x||=1} x^T X x \geq x^T Y x \geq \min_{||y||=1} y^T Y y = \lambda_{min}(Y) \tag{4.47}$$

To prove the main result, let us recall the two designs we are comparing. The "mismatched LQR" is designed by solving the Riccati Equation

$$PA_0 + A_0^T P - \frac{1}{\rho} PBB^T P + Q_0 = 0 \tag{4.48}$$

and has the associated Frequency Domain Equality

$$[I + G_0\Phi(-s)B]^T[I + G_0\Phi(s)B] = I + \frac{1}{\rho} B^T\Phi^T(-s)Q_0\Phi(s)B \tag{4.49}$$

where this FDE is derived in the same manner as the robust FDE.

The RLQR is designed by solving the modified Riccati Equation

$$PA_0 + A_0^T P - \frac{1}{\rho} PBB^T P + Q_0 + \frac{1}{\gamma} PLL^T P + \gamma NN^T = 0 \tag{4.50}$$

and has the associated robust FDE:

$$[I+G\Phi(-s)B]^T[I+G\Phi(s)B] = I+\frac{1}{\rho} B^T\Phi^T(-s)[P(A_0-A)+(A_0^T-A^T)P+Q]\Phi(s)B \tag{4.51}$$

Theorem 4.2 *The maximum singular value of the sensitivity function of the actual plant with the RLQR design is always less than or equal to the maximum singular value of the sensitivity of the same plant with the mismatched LQR design at any given frequency.*

Proof 4.2 *Let us subtract (4.51) from (4.49):*

$$[I + G_0\Phi(-s)B]^T[I + G_0\Phi(s)B] - [I + G\Phi(-s)B]^T[I + G\Phi(s)B]$$

$$= \frac{1}{\rho}B^T\Phi^T(-s)[Q_0 - Q_0 - P(A_0 - A) - (A_0^T - A^T)P]\Phi(s)B \tag{4.52}$$

Substituting $A = A_0 + \sum_{i=1}^{p} q_i E_i$ *and the Riccati Equations (4.48) and (4.50), algebraic manipulations produce*

$$[I + G_0\Phi(-s)B]^T[I + G_0\Phi(s)B] - [I + G\Phi(-s)B]^T[I + G\Phi(s)B]$$

$$= \frac{1}{\rho}B^T\Phi^T(-s)[P\sum_{i=1}^{p} q_i E_i + \sum_{i=1}^{p} q_i E_i^T P - \gamma NN^T - \frac{1}{\gamma}PLL^TP]\Phi(s)B \tag{4.53}$$

Since N *and* L *were chosen such that*

$$P\sum_{i=1}^{p} q_i E_i + \sum_{i=1}^{p} q_i E_i^T P \leq \gamma NN^T + \frac{1}{\gamma}PLL^TP \tag{4.54}$$

it is clear that

$$P\sum_{i=1}^{p} q_i E_i + \sum_{i=1}^{p} q_i E_i^T P - \gamma NN^T - \frac{1}{\gamma}PLL^TP \leq 0 \tag{4.55}$$

Thus the right hand side of (4.53) is negative definite, which implies

$$[I + G_0\Phi(-s)B]^T[I + G_0\Phi(s)B] \leq [I + G\Phi(-s)B]^T[I + G\Phi(s)B] \tag{4.56}$$

Using Lemma 4.1, we see that

$$\lambda_{min}([I + G_0\Phi(-s)B]^T[I + G_0\Phi(s)B]) \leq \lambda_{min}([I + G\Phi(-s)B]^T[I + G\Phi(s)B]) \tag{4.57}$$

$$\Longleftrightarrow \sigma_{min}(I + G_0\Phi(s)B]) \leq \sigma_{min}(I + G\Phi(s)B]) \tag{4.58}$$

$$\Longleftrightarrow \sigma_{max}\left\{(I + G_0\Phi(s)B])^{-1}\right\} \geq \sigma_{max}\left\{(I + G\Phi(s)B])^{-1}\right\} \tag{4.59}$$

Equation (4.59) is the result we desired, since this equation says that the maximum singular value of the sensitivity function of the mismatched LQR design is greater than that of the RLQR design at every frequency. This implies greater performance robustness in the RLQR design.

As an example, let us look at typical sensitivity plots for the benchmark problem of figure 3-1. This is a single input-single output system, so the maximum singular value of the sensitivity function is equal to the magnitude of the sensitivity function. We calculated the sensitivity function for the system with $k = 2$, and with the gains listed in Appendix B.1. For comparison, we also calculated the sensitivity function for the RLQR design with $\gamma = .5$.

The representative plots are shown in figure 4-1. Note that since the LQR design is "mismatched", we are not guaranteed that the sensitivity function is less than 1 for all frequencies. Also notice that we have increased performance robustness with $\gamma = .5$ compared to $\gamma = 1$, although in general one value of γ will not necessarily have better performance robustness over all frequencies compared to another value of γ.

We have also plotted the corresponding complimentary sensitivity functions in figure 4-2. Notice that the RLQR designs have a higher bandwidth than the mismatched LQR design, which implies that we are more sensitive to unstructured uncertainty. Also, the affect of γ on bandwidth is evident, as in this case the design with $\gamma = .5$ has a higher bandwidth, and thus is less robust to high-frequency unstructured uncertainty.

4.5 Conservatism

The RLQR design is definitely conservative with respect to stability robustness. That is, if we can design an RLQR controller by finding a solution to the RLQR Riccati equation (2.32), then we have guaranteed that the uncertain system is stable. However,

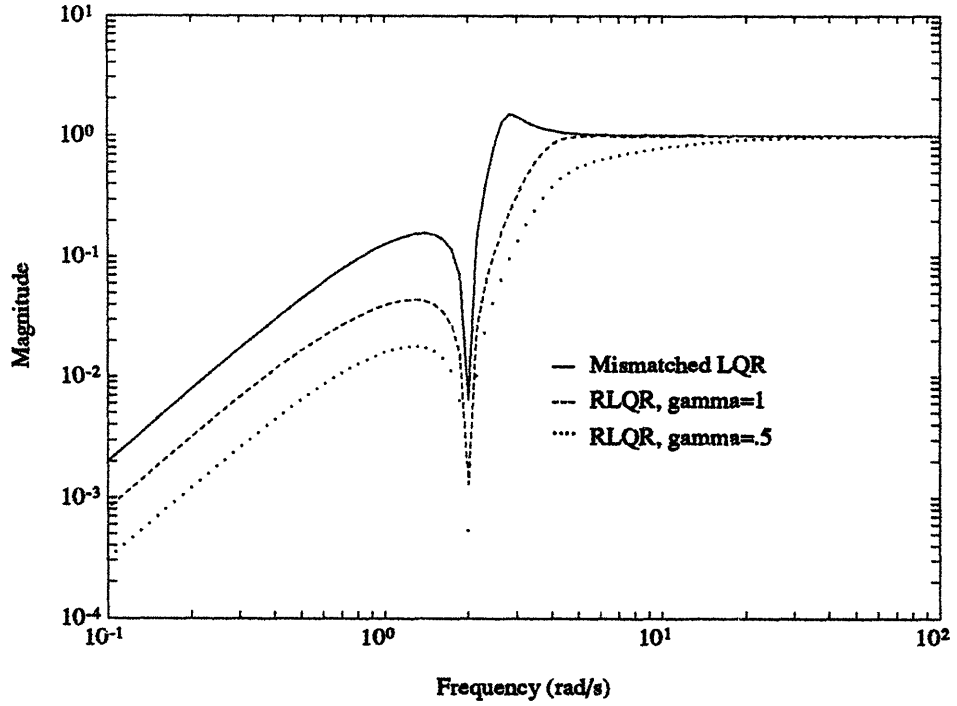

Figure 4-1: Typical sensitivity plots of the benchmark problem with $k = 2$.

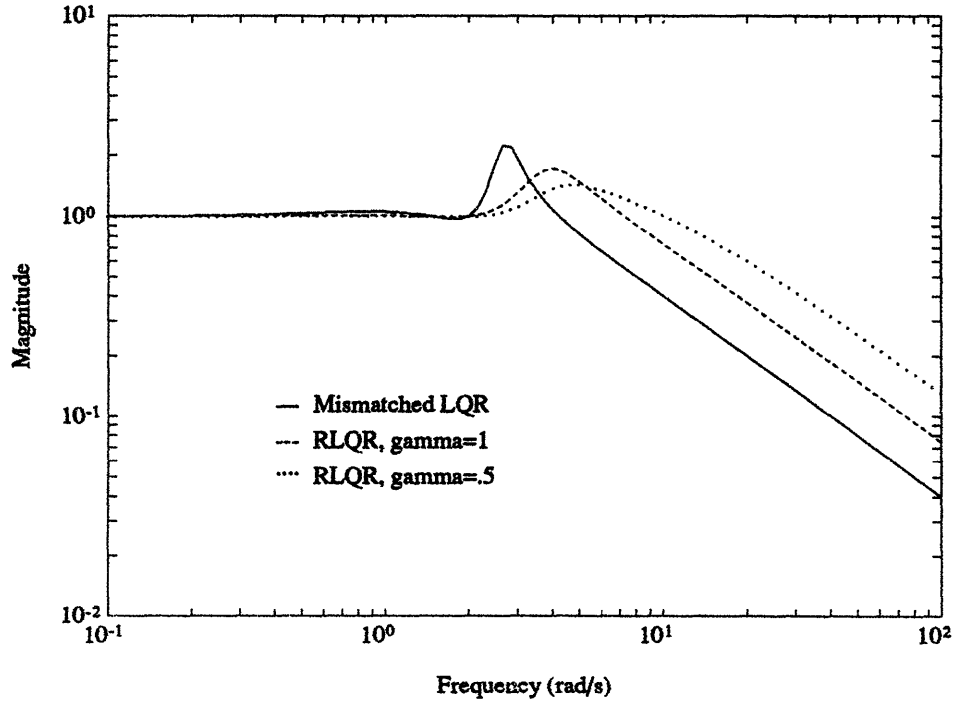

Figure 4-2: Typical sensitivity plots of the benchmark problem with $k = 2$.

not being able to find a solution to (2.32) does not imply that we can not find stabilizing gains (though finding stabilizing gains does not imply we have found gains which will give us the same performance as an RLQR design).

This section will try to quantify the ways in which the design is conservative.

4.5.1 Level of Conservatism

To understand the conservatism of the RLQR design, we will compare it to the well-known "Small Gain Theorem."

In section 2.1, we have modelled our uncertain system as

$$\dot{x}(t) = (A_0 + \sum_{i=1}^{p} q_i l_i n_i^T)x(t) + Bu(t) \tag{4.60}$$

We can equivalently write this system as

$$\dot{x}(t) = A_0 x(t) + L\Delta N^T x(t) + Bu(t) \tag{4.61}$$

where $\Delta = diag(q_1, q_2, ..., q_p)$, and L and N are defined as in equation (2.29):

$$L = [l_1\ l_2\ l_3 \ldots]; \qquad N = [n_1\ n_2\ n_3 \ldots] \tag{4.62}$$

After designing an RLQR controller, the closed loop system becomes

$$\dot{x}(t) = (A_0 - BG)x(t) + L\Delta N^T x(t) \tag{4.63}$$

where $G = \frac{1}{\rho}B^T P$, P is the solution of the RLQR Riccati equation (2.32).

Note that all the uncertainty of the system is in the Δ matrix. Thus we can seperate the "uncertain" part of the system, as shown in figure 4-3.

With the above framework in mind, Obradovic [22] showed that the Petersen-Hollot overbounding procedure, used in section 2.3.3, is just as conservative as the following

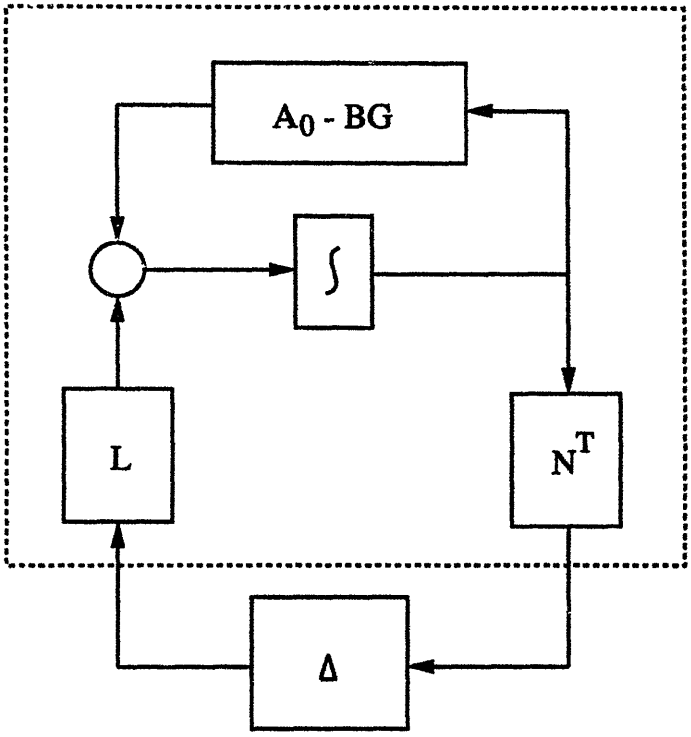

Figure 4-3: System with Uncertainty Seperated from the plant

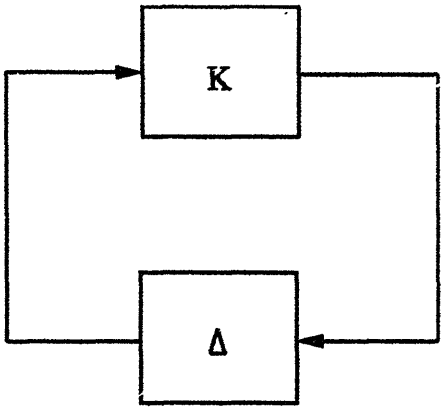

Figure 4-4: The Structure of the Small Gain Theorem

"Small Gain Theorem":

Theorem 4.3 *Given a plant K with an uncertainty Δ, $\|\Delta\|_\infty \leq 1$, as shown in figure 4-4, then a sufficient condition for the system to be stable is $\|K\|_\infty < 1$.*

Note that since $\Delta = diag(q_1, q_2, ..., q_p)$, $|q_i| \leq 1$, we satisfy the condition $\|\Delta\|_\infty \leq 1$. Obradovic showed that the Small Gain Theorem is satisfied for our system in figure 4-3 if and only if the Riccati equation which results from the Petersen-Hollot bounding procedure has a solution $P = P^T > 0$. Thus there is a one-to-one correspondence between the Petersen-Hollot bounds and the Small Gain Theorem.

Notice that the Small Gain Theorem is only a sufficient condition for stability. This is because it does not take into account the structure of the Δ matrix. In our system, Δ has a very special structure; it is diagonal. The Small Gain Theorem guarantees stability for all possible Δ matrices satisfying $\|\Delta\|_\infty \leq 1$, and not just diagonal matrices. Thus, we are compensating for modelling errors which do not exist. (But recall that we are interested in not only stability, but also performance).

4.5.2 Factorization

We have seen that the assumption that the uncertainty matrices E_i are rank 1 is valid for our mass-spring-dashpot systems. However, system identification techniques are often formulated such that this will not hold; the parameters we identify with uncertainty regions result in matrices which are rank 2.

In the case where this is not true, we must consider each E_i as a sum of rank 1 matrices. This will lead to additional conservatism. The system will try to compensate for two parameters which vary independently, when actually it is only one uncertain parameter.

To make this more clear, let us look at a simple acedamic example. Let us assume we are looking at a system with two complex conjugate poles, where the frequency of the pole is uncertain, and can vary independant of the known value of the damping. While there is not necessarily a system with such a physical parameter which causes this particular variation, it will demonstrate the type of conservatism that results when the rank 1 assumption is violated.

Our system matrix will be of the form

$$A = \begin{bmatrix} \sigma_0 & \omega_0 + \Delta \\ -\omega_0 - \Delta & \sigma_0 \end{bmatrix} \qquad |\Delta| \leq 1 \tag{4.64}$$

In this case, we must break the uncertainty into the two matrices

$$E_1 = \begin{bmatrix} 0 & 1 \\ 0 & 0 \end{bmatrix} \qquad E_2 = \begin{bmatrix} 0 & 0 \\ -1 & 0 \end{bmatrix} \tag{4.65}$$

But this is equivalent to considering the following uncertain system:

$$A = \begin{bmatrix} \sigma_0 & \omega_0 + \Delta_1 \\ -\omega_0 - \Delta_2 & \sigma_0 \end{bmatrix} \qquad |\Delta_i| \leq 1 \tag{4.66}$$

Here, Δ_1 and Δ_2 are independent perturbations. Thus we are designing a controller for the case when the two poles are not complex conjugates, which is physically impossible. Similarly, in physical systems when a parameter has a rank 2 uncertainty matrix, we must seperate the uncertainty into two parameters, and then the RLQR design is compensating for situations which are physically impossible.

Some extensions of the Petersen-Hollot bounds have been proposed to alleviate this problem. For instance, see [23]. However, all attempted extensions are just as conservative as assuming we have rank 1 matrices. Thus, our assumption may impose additional conservatism.

4.5.3 Worst-Case Disturbance

We can write the uncertain system matrix as

$$A = A_0 + L\Delta N^T \tag{4.67}$$

where $\Delta = diag(q_1, q_2, ..., q_p)$. Thus, we can consider the system as:

$$\dot{x}(t) = A_0 x(t) + L\Delta N^T x(t) + Bu(t) \tag{4.68}$$

If we consider the term $\Delta N^T x(t)$ as a disturbance $d(t)$, we can write the system equations as

$$\dot{x}(t) = A_0 x(t) + Ld(t) + Bu(t) \tag{4.69}$$

Now, an $\mathcal{H}_\infty$ design on the system will find the "worst-possible" $d(t)$ [12]. This will turn out to be of the form

$$d^*(t) = \frac{1}{\gamma} L^T P x(t) \tag{4.70}$$

where P is the solution of the $\mathcal{H}_\infty$ Riccati equation

$$PA_0 + A_0^T P + Q_0 - P(\frac{1}{\rho} BB^T - \frac{1}{\gamma} LL^T)P = 0 \tag{4.71}$$

We have noted that in the equivalent cost functional (4.3), we are finding a "worst-case" disturbance. But this worst-case disturbance may not be in the form of $\Delta N^T x(t)$. To demonstrate this, let us look at the benchmark problem of figure 3-1. With the same choices of Q_0, ρ, and γ as in section 3.1.1, the solution P to (4.71) is

$$P = \begin{bmatrix} .3155 & .1698 & .0939 & .4152 \\ .1698 & .7913 & .0254 & .4549 \\ .0939 & .0254 & .0437 & .1070 \\ .4152 & .4549 & .1070 & .6666 \end{bmatrix} \tag{4.72}$$

so that the value of $\frac{1}{\gamma}L^T P$ is

$$\frac{1}{\gamma}L^T P = \begin{bmatrix} -.2783 & -.3719 & -.0548 & -.4846 \end{bmatrix} \tag{4.73}$$

and the worst case disturbance, d^*, is

$$d^*(t) = -.2783x_1(t) - .3719x_2(t) - .0548x_3(t) - .4846x_4(t) \tag{4.74}$$

However, the "actual disturbances" in the system are

$$\Delta N^T x(t) = q \begin{bmatrix} -.866 & .866 & 0 & 0 \end{bmatrix} x(t) = -.866qx_1(t) + .866qx_2(t) \tag{4.75}$$

For any value of q such that $|q| \leq 1$, we see the actual value of the disturbance as a function of time will not be the worst-case disturbance.

Thus we see that we are adding some conservatism on the design by accounting for equivalent disturbances which may not exist.

4.5.4 No Solution

We have shown that the RLQR design is a conservative one with respect to stability robustness. This means that if we can design an RLQR controller for a system with

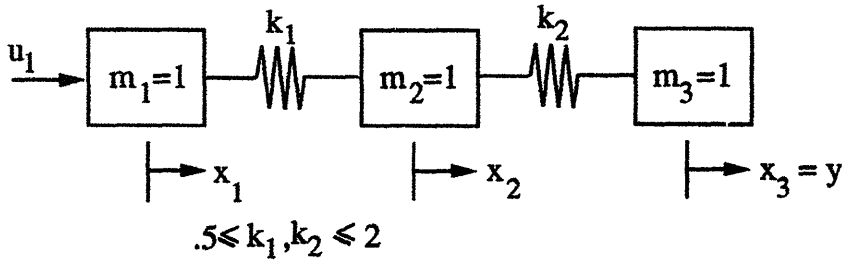

Figure 4-5: Example with No RLQR solution

parametric uncertainty, then we will guarantee the stability of that system for all values of the uncertain parameters. However, we may not be able to design an RLQR controller when stabilizing gains do exist; that is, the RLQR Riccati equation (2.32) may not have a solution for any value of γ but we can still stabilize the system. For a discussion of when solutions exist to these type of Riccati equations, see [25].

As an example, let's look at the 2 uncertain spring example of section 3.3. But now assume that we have only one control, as shown in figure 4-5. We have chosen our parameters ρ and Q_0 as:

$$\rho = .01 \qquad Q_0 = \begin{bmatrix} 0 & 0 & 0 & 0 & 0 & 0 \\ 0 & 0 & 0 & 0 & 0 & 0 \\ 0 & 0 & 1 & 0 & 0 & 0 \\ 0 & 0 & 0 & 0 & 0 & 0 \\ 0 & 0 & 0 & 0 & 0 & 0 \\ 0 & 0 & 0 & 0 & 0 & 0 \end{bmatrix} \tag{4.76}$$

We could not find a solution to the RLQR Riccati equation (2.32) for this choice of ρ and Q_0, and for any choice of the factorization of the E_i matrices. In fact, even the mismatched LQR design is not stable for all values of the uncertain springs.

However, gains do exist which stabilize the system; one such gain is

$$G = \begin{bmatrix} 7.3804 & 1.8252 & 0.7944 & 3.8420 & 10.4976 & 8.9988 \end{bmatrix} \tag{4.77}$$

These gains were found by trial and error, and tested with an exhaustive search over the possible values of the uncertain stiffness values. They actually correspond to an LQR design with the same values of ρ and Q_0, but with a design system corresponding with $k_1 = .875$ and $k_2 = 1.25$ in figure 4-5.

So this is an example of when we can not find a solution to the RLQR Riccati equation (2.32), but when stabilizing gains so exist.

4.6 Summary

We have derived and explained the properties of the RLQR controller. We gain stability and performance robustness by minimizing a weighted sum of the uncertain energies in the system, and also consider "worst-case" disturbances acting in the direction of the uncertainty. We have also shown that we have gained better disturbance rejection guarantees than LQR designs. These properties are due to the higher gains in RLQR designs, which effectively adds more damping to the system. However, the price we pay is a higher bandwidth, and therefore less robustness to high-frequency unstructured uncertainty.

This uncertain energy minimization appears to be the key to controlling a parametrically uncertain system. We are able to minimize the effects of uncertain energy because we could directly measure all states of the system. The problem would be much more difficult if, for example, we could only measure y, the position of the second mass in the benchmark problem. The controller can not minimize the energy unless it can measure it in some way. Thus, the output feedback problem is a much more difficult one.

The price we pay for the RLQR design is a high degree of conservatism, and a higher bandwidth. This higher bandwidth implies less robustness to high-frequency unstruc-

tured uncertainty.

These properties of the RLQR design will hopefully guide us in designing robust controllers using only output feedback.

Chapter 5

Conclusions

In this chapter we will summarize the main results of this thesis, and describe some of the next steps in the evolution of a robust controller.

5.1 Contributions

We have presented an extension of the standard LQR called the robust LQR (RLQR). It is derived using an overbounding technique known as Petersen-Hollot bounds. The result of this overbounding is a guarantee of stability in the presence of parametric uncertainty, and also guaranteed robustness in terms of gain and phase margins. The resulting full-state controller is designed by solving a single Riccati-type equation. This Riccati Equation is identical to ones which have appeared in the literature with this overbounding method.

The novelty presented in the derivation was the interpretation of the controller as an extension of LQR. In fact, we have shown that the RLQR design is equivalent to an LQR design with an extremely intelligent choice of the state weighting matrix, or a modified full-state $\mathcal{H}_2/\mathcal{H}_\infty$ design. It is this choice of the state weighting matrix which makes the system robust to parametric uncertainty.

To understand the properties of the RLQR, we have conducted simulations for some

simple systems. These systems consisted of masses connected by springs with unknown stiffness. Several different configurations were examined, and in all of them the RLQR design appeared to be reducing the unknown potential energies stored in the springs, so as to mitigate their effect on the dynamics of the system. The effect of additional control variables was additional performance robustness. Other simulations showed that the RLQR design was able to attenuate disturbances, even better than a "mismatched" LQR design.

We were then able to show analytically how the choice of the "equivalent state weighting matrix" added robustness to the system. In the standard LQR design, we minimize a cost functional which contains quadratic weights on the states and on the control. In the RLQR design, the state weighting matrix adds two more quadratic terms to this cost functional. The first is equivalent to the stored potential energy of the springs. The second is a term which is the same as a worst-case disturbance in the direction of the uncertain parameters. These two terms were sufficient to guarantee robustness to the parametric uncertainty, as well as some additional robustness guarantees stated earlier. However, the RLQR design has a higher bandwidth, which we can adjust by trading the relative weighting of these two additional items in the cost functional.

These interpretations were shown to generalize to structural systems with uncertain stiffness and damping elements. With uncertain stiffness elements, we are minimizing a weighted sum of the uncertain potential energy stored in each element. For uncertain damping elements, we are minimizing a weighted sum of the rate of dissipation of energy through each element. In either case, we are minimizing the impact of the uncertain elements on the stability and performance of the system.

We were able to show that the RLQR design attenutated disturbances better than a mismatched LQR design. We were then able to show that in fact we are guaranteed to have better performance in the RLQR design, because the maximum singular value of the RLQR sensitivity function is always smaller than that of the standard LQR design.

One of the prices we pay for this robustness to parametric uncertainty is that the

design is very conservative with respect to stability robustness. In fact, we showed that it is at least as conservative as the Small Gain Theorem. The result of this conservatism is that there may be no RLQR controller for a given system, even when stabilizing gains do exist.

In summary, we have examined a full-state controller which is robust to parametric uncertainty. It achieves its performance robustness by minimizing the effect of uncertain stored energy and uncertain dissipated power. However, it is a high-bandwidth design.

5.2 Future Work

Before this control technique can be implemented on a real system, several extensions need to be made. Throughout this thesis, we have assumed complete knowledge of all state variables in the system. In a real structure, this is impossible. Thus, we need to extend the results to the case of output feedback, when only some of the states are available.

One possible scheme for output feedback would be to create the dual to the robust LQR. This would be a model-based observer, which would estimate the state of the system based upon the output measurements and knowledge of a model of the system. A basic problem with this scheme is that the model of the system is uncertain, and thus our observer will not necessarily be matched to the system. Research should be done in this area to determine possible methods for compensating for this problem.

Another assumption throughout this thesis was that the uncertain parameters were known to be within a bounded interval. To actually implement a robust controller, a method of determining these bounds must be found for real systems. This is a question of system identification. We need to determine how system identification techniques can be used to help in robust control.

We would also like to extend the results to more general types of uncertainty. For instance, we would like to remove the "rank 1" assumption on the uncertainty matrices.

This would require an extension of the Petersen-Hollot bounds. The types of uncertainty we must examine in real systems are the ones which are a result of the system identification; that is, if we can use system identification to determine one type of uncertainty, we must adapt the robust control techniques to handle this uncertainty. Preliminary results show that system identification techniques on large space structures may result in uncertainty matrices which are rank 2. Thus an extension of the overbounding technique is needed.

Finally, we would like to actually design and implement a robust controller on a large space system. Such a system has uncertainty in modal frequencies and damping values, and thus we can immediately see the need for a robust controller.

So although a deeper understanding of how to robustify a system has been achieved, much work needs to be done to design and implement robust controllers.

Appendix A

Applying LQR to an Uncertain System

This appendix presents an example of the fact that classical LQR methods do not necessarily imply closed-loop stability for open-loop stable plants with uncertain parameters.

Let us consider the system of the form

$$\dot{x}(t) = Ax(t) + Bu(t) \tag{A.1}$$

$$y(t) = Cx(t) \tag{A.2}$$

with the values

$$A = \begin{bmatrix} 0 & 1 & 0 & 0 & 0 & 0 \\ 0 & 0 & 1 & 0 & 0 & 0 \\ 0 & 0 & 0 & 1 & 0 & 0 \\ 0 & 0 & 0 & 0 & 1 & 0 \\ 0 & 0 & 0 & 0 & 0 & 1 \\ -4 & -a_1 & -164.8186 & -a_3 & -40 & -a_5 \end{bmatrix} \qquad B = \begin{bmatrix} 0 \\ 0 \\ 0 \\ 0 \\ 0 \\ 1 \end{bmatrix} \tag{A.3}$$

$$C = \begin{bmatrix} .5 & 1.5 & 1 & 0 & 0 & 0 \end{bmatrix} \tag{A.4}$$

with the uncertain parameters bounded by

$$a_5 \in \begin{bmatrix} 10, & 12 \end{bmatrix} \tag{A.5}$$

$$a_3 \in \begin{bmatrix} 82.875, & 90 \end{bmatrix} \tag{A.6}$$

$$a_1 \in \begin{bmatrix} 7.1171, & 126.2908 \end{bmatrix} \tag{A.7}$$

This system has the characteristic function given by

$$s^6 + a_5 s^5 + 40 s^4 + a_3 s_3 + 164.8186 s^2 + a_1 s + 4 \tag{A.8}$$

and thus it is simple to check with Kharitonov's Theorem [3] that this system is indeed stable regardless of the values of the uncertain parameters.

For a nominal system, let us pick

$$a_5 = 10 \qquad a_3 = 90 \qquad a_1 = 7.1171 \tag{A.9}$$

Though this is not the "midpoint" of the intervals, it will demonstrate the basic principle. It is quite likely that we could find an example with the nominal system at the midpoint if we go to a higher order system.

For design, we choose

$$\rho = 10 \qquad Q_0 = C^T C \tag{A.10}$$

The resulting LQR gains are given by

$$G = \begin{bmatrix} .0031 & .1162 & .0641 & .0287 & .0072 & .0007 \end{bmatrix} \tag{A.11}$$

It is easy to check that the closed loop system is not stable for all values of the

parameters in (A.5)-(A.7). Thus we see that examples do exist where an LQR design does not guarantee stability. Such examples are not easy to find for systems with such a low order. Higher order examples should be easier to find since there are more degrees of freedom.

Appendix B

Simulation Control Gains and Closed-Loop Poles

This appendix will list the control gains and closed loop poles for various values of the spring constant(s) from each of the simulations in Chapter 2.

B.1 Benchmark Problem (c.f. 3.1.1)

Mismatched LQR Design gains ($k = 1.25$):

$$G = \begin{bmatrix} 8.0902 & 1.9098 & 4.0225 & 8.9945 \end{bmatrix} \tag{B.1}$$

RLQR Design gains:

$$G = \begin{bmatrix} 25.5316 & -1.2656 & 7.4831 & 33.1313 \end{bmatrix} \tag{B.2}$$

Note that some of the RLQR gains are significantly larger than the mismatched LQR gains. Also notice that the second RLQR gain, the one that multiplies the position of m_2, is negative. This implies that the RLQR magnifies the displacement of mass m_2. This does not cause instability due to the large gains on the other state variables.

Closed-Loop Poles:

k	Mismatched LQR	RLQR
.5	-1.7089 $\pm$ 1.8164j	-3.3448 $\pm$ 3.0737j
	-0.3023 $\pm$ 0.8441j	-0.3967 $\pm$ 0.6562j
.875	-1.2977 $\pm$ 1.4828j	-2.8644 $\pm$ 2.7733j
	-0.7135 $\pm$ 1.3208j	-0.8771 $\pm$ 0.7526j
1.25	-1.4406 $\pm$ 0.8152j	-1.9798 $\pm$ 2.7396j
	-0.5706 $\pm$ 2.0583j	-2.4316
		-1.0918
1.625	-1.5911 $\pm$ 0.4605j	-1.4386 $\pm$ 3.2035j
	-0.4201 $\pm$ 2.3971j	-3.7540
		-0.8518
2	-0.3154 $\pm$ 2.6564j	-1.1533 $\pm$ 3.5826j
	-1.9806	-4.3973
	-1.4111	-0.7791

Note that the significant damping has been added to the poles in the RLQR design. Also, the frequency of the closed loop poles is farther away from the uncertain value of the open-loop pole (c.f. 3.2), which is in the range $\omega = 1$ to $\omega = 2$.

B.2 Benchmark Problem with Additional Control Variable (c.f. 3.1.2)

Mismatched LQR Design gains ($k = 1.25$):

$$G = \begin{bmatrix} 0.5174 & -0.3192 & 1.0025 & 0.1726 \\ 1.2150 & 8.7831 & 0.1726 & 4.1876 \end{bmatrix} \tag{B.3}$$

RLQR Design gains:

$$G = \begin{bmatrix} 6.8354 & -2.7445 & 3.6621 & -0.6306 \\ -2.4089 & 11.5444 & -0.6306 & 4.7866 \end{bmatrix} \tag{B.4}$$

Once again, some of the gains are larger, and the others have the opposite sign. Due to the extra control variable, the magnitude of the control gains, in both designs, is reduced.

Closed-Loop Poles:

k	Mismatched LQR	RLQR
.5	-2.1090 $\pm$ 2.2001j	-2.5331 $\pm$ 2.6712j
	-0.4861 $\pm$ 0.9185j	-1.6912 $\pm$ 1.7213j
.875	-2.0936 $\pm$ 2.2779j	-2.5288 $\pm$ 2.7950j
	-0.5015 $\pm$ 1.0936j	-1.6955 $\pm$ 1.7404j
1.25	-2.0721 $\pm$ 2.3545j	-2.5236 $\pm$ 2.9155j
	-0.5230 $\pm$ 1.2343j	-1.7007 $\pm$ 1.7555j
1.625	-2.0452 $\pm$ 2.4304j	-2.5181 $\pm$ 3.0329j
	-0.5498 $\pm$ 1.3523j	-1.7062 $\pm$ 1.7676j
2	-2.0136 $\pm$ 2.5061j	-2.5127 $\pm$ 3.1473j
	-0.5815 $\pm$ 1.4534j	-1.7116 $\pm$ 1.7773j

The RLQR design has higher damping than the mismatched LQR design. Note that with the additional control, the pole locations are almost identical in the RLQR design for all values of the stiffness k.

B.3 Benchmark Problem with Control at Output (c.f. 3.2)

Mismatched LQR Design gains ($k = 1.25$):

$$G = \begin{bmatrix} 0.7295 & 9.2705 & 1.0165 & 4.3059 \end{bmatrix} \tag{B.5}$$

RLQR Design gains:

$$G = \begin{bmatrix} -15.6044 & 32.4151 & 41.2569 & 8.5358 \end{bmatrix} \tag{B.6}$$

The magnitudes of the RLQR gains are much larger in this example. Also, note that we are magnifying the position error of m_1 in this case.

Closed-Loop Poles:

k	Mismatched LQR	RLQR
.5	-2.130 ± 2.2397j	-3.8457 ± 3.4373j
	-0.0226 ± 0.7230j	-0.4222 ± 0.3710j
.875	-2.1083 ± 2.3024j	-3.3480 ± 3.1530j
	-0.0447 ± 0.9465j	-0.5317
		-1.3081
1.25	-2.0821 ± 2.3633j	-2.5334 ± 3.0999j
	-0.0709 ± 1.1203j	-0.4317
		-3.0372
1.625	-2.0521 ± 2.4227j	-1.9316± 3.4878j
	-0.1008 ± 1.2656j	-0.4025
		-4.2702
2	-2.0184 ± 2.4810j	-1.5907 ± 3.8632j
	-0.1345 ± 1.3918j	-0.3878
		-4.9665

The RLQR has added significant damping, and also moved the poles away from the uncertain pole frequency, $\omega = 1$ to $\omega = 2$.

B.4 Two Spring Example (c.f. 3.3)

Mismatched LQR Design gains ($k_1 = k_2 = 1.25$):

$$G = \begin{bmatrix} 0.5177 & -0.4232 & -0.2056 & 1.0005 & 0.1854 & -0.3413 \\ 1.2696 & 6.3750 & 2.3548 & 0.1854 & 3.5659 & 8.9512 \end{bmatrix} \tag{B.7}$$

RLQR Design gains:

$$G = \begin{bmatrix} 8.2237 & 3.7014 & -2.3270 & 4.1559 & 0.6094 & 12.7251 \\ 1.1708 & 27.6731 & -1.9246 & 0.6094 & 7.8550 & 36.9120 \end{bmatrix} \tag{B.8}$$

In this case, the two control variables allow the RLQR design to have control gains whose magnitudes are comparable to the mismatched LQR gains, even though there are two uncertain springs.

Closed-Loop Poles:

k_1	k_2	Mismatched LQR	RLQR
.5	.5	-1.4778 ± 1.6313j	-3.5473 ± 3.2032j
		-0.4757 ± 1.1173j	-2.0647 ± 2.0869j
		-0.3296 ± 0.7806j	-0.3934 ± 0.6522j
.5	2	-0.1318 ± 2.7163j	-1.3752 ± 3.6575j
		-0.4601 ± 0.8851j	-1.8599 ± 2.1660j
		-1.9597	-0.7693
		-1.4230	-4.7714
1.25	.5	-1.4044 ± 1.8988j	-3.5238 ± 3.3098j
		-0.5740 ± 1.2369j	-2.0890 ± 2.2574j
		-0.3048 ± 0.8714j	-0.3926 ± 0.6514j
1.25	1.25	-0.4815 ± 2.2483j	-2.4036 ± 3.1766j
		-0.4778 ± 1.2330j	-1.6674 ± 2.0081j
		-1.3239 ± 0.7986j	-2.8201
			-1.0488
1.25	2	-0.2100 ± 2.7685j	-1.4766 ± 3.6580j
		-0.4939 ± 1.2405j	-1.7957 ± 2.4290j
		-1.5792 ± 0.2806j	-0.7667
			-4.6994
2	.5	-1.3115 ± 2.1799j	-3.4873 ± 3.4186j
		-0.6693 ± 1.3015j	-2.1261 ± 2.4011j
		-0.3024 ± 0.9021j	-0.3919 ± 0.6509j
2	2	-0.3158 ± 2.8378j	-1.6205 ± 3.6685j
		-0.4715 ± 1.5370j	-1.6830 ± 2.6634j
		-1.4959 ± 0.3794j	-4.6391
			-0.7647

We again see much more damping in the RLQR design than in the mismatched LQR design.

B.5 Partially Known System (c.f. 3.4)

Mismatched LQR Design gains ($k_1 = 1.25$):

$$G = \begin{bmatrix} 0.5177 & -0.4232 & -0.2056 & 1.0005 & 0.1854 & -0.3413 \\ 1.2696 & 6.3750 & 2.3548 & 0.1854 & 3.5659 & 8.9512 \end{bmatrix} \tag{B.9}$$

RLQR Design gains:

$$G = \begin{bmatrix} 6.8601 & -1.3862 & -1.4464 & 3.6912 & -0.4745 & 3.5000 \\ -2.3532 & 10.2218 & 1.2952 & -0.4745 & 4.5172 & 8.2181 \end{bmatrix} \tag{B.10}$$

The mismatched LQR gains are the same as those for the two uncertain spring example, since the nominal system is the same. However, the magnitude of the RLQR gains has been significantly reduced, since there is less uncertainty in the system.

Closed-Loop Poles:

k_1	Mismatched LQR	RLQR
.5	-0.3417 ± 2.1847j	-2.1751 ± 2.4874j
	-0.4528 ± 0.8709j	-0.5854 ± 1.8620j
	-1.4887 ± 0.7117j	-1.3438 ± 0.7527j
.875	-0.4027 ± 2.2111j	-2.1823 ± 2.6425j
	-0.4770 ± 1.0558j	-0.5809 ± 1.8561j
	-1.4035 ± 0.7782j	-1.3410 ± 0.7497j
1.25	-0.4815 ± 2.2483j	-2.1891 ± 2.7878j
	-0.4778 ± 1.2330j	-0.5764 ± 1.8514j
	-1.3239 ± 0.7986j	-1.3387 ± 0.7473j
1.625	-0.5772 ± 2.3090j	-2.1955 ± 2.9250j
	-0.4395 ± 1.3872j	-0.5721 ± 1.8477j
	-1.2665 ± 0.7903j	-1.3367 ± 0.7455j
2	-0.6730 ± 2.4035j	-2.2013 ± 3.0553j
	-0.3788 ± 1.4955j	-0.5680 ± 1.8448j
	-1.2314 ± 0.7741j	-1.3350 ± 0.7440j

Since we have the same mismatched control gains as section B.4, we will have the same closed-loop poles (with $k_2 = 1.25$). However, we gain added robustness in the RLQR design. Note that there is little variation in the closed-loop poles of this system, with two control variables and only one uncertain spring.

References

[1] M. Athans. *Lecture Notes for 6.234J.* Massachusetts Institue of Technology, Jan 1990.

[2] B.R. Barmish. "A Generalization of Kharitonov's Four Polynomial Concept for Robust Stability Problems with Linearly Dependent Coefficient Perturbations". *Proc. 1988 American Control Conference, Atlanta, GA*, pp. 1869–1875, June 1988.

[3] B.R. Barmish. "New Tools for Robustness Analysis". *Proc. 1988 Conference on Decision and Control, Austin, TX*, pp. 1–6, December 1988.

[4] B.R. Barmish and R. Tempo. "The Robust Root Locus". *Proc. 1988 Conference on Decision and Control, Austin, TX*, pp. 1386–1391, December 1988.

[5] A.C. Bartlett, C.V. Hollot, and H. Lin. "Root Locations of an Entire Polytope of Polynomials: It Suffices to Check the Edges". *Proc. 1987 American Control Conference, Minneapolis, MN*, pp. 1611–1616, June 1987.

[6] D. S. Bernstein. "Robust Static and Dynamic Output-Feedback Stabilization: Deterministic and Stochastic Perspectives". *IEEE Trans. on Auto. Control*, 32(12), pp. 1072–1084, December 1987.

[7] D. S. Bernstein and W. M. Haddad. "The Optimal Projection Equations with Petesen-Hollot Bounds: Robust Stability and Performance Via Fixed-Order Dy-

namic Compensation for Systems with Sructured Real-Valued Parameter Uncertainty". *IEEE Trans. on Auto. Control*, 33(6), pp. 578–582, June 1988.

[8] D. S. Bernstein and W. M. Haddad. "Robust Stability and Performance via Fixed-Order Dynamic Compensation with Guaranteed Cost Bounds". *Mathematics of Control, Signals, and Systems*, 3(2), pp. 139–163, 1990.

[9] D. S. Bernstein and D.C. Hyland. "Optimal Projection for Uncertain Systems (OPUS): A Unified Theory of Reduced-Order, Robust Control Design". In S.N. Atturi and A.K. Amos, editors, *Large Space Structres: Dynamics and Control*, pp. 263–302. Spring-Verlag, 1988.

[10] H. Chapellat and S. Bhattacharyya. "A Generalization of Kharitonov's Theorem: Robust Stability of Interval Plants". *IEEE Trans. on Auto. Control*, 34(3), pp. 306–311, March 1989.

[11] S. Dasgupta. "A Kharitonov Like Theorem for Systems Under Nonlinear Passive Feedback". *Proc. 1987 Conference on Decision and Control, Los Angelos, CA*, pp. 2062–2063, December 1987.

[12] J. Doyle, K. Glover, P. Khargonekar, and B. Francis. "State-Space Solutions to Standard $\mathcal{H}_2$ and $\mathcal{H}_\infty$ Control Problems". *IEEE Trans. on Auto. Control*, 34(8), pp. 831–847, August 1989.

[13] W. M. Haddad and D. S. Bernstein. "Robust, Reduced-Order, Nonstrictly Proper State Estimation via the Optimal Prjoection Equations with Petersen-Hollot Bounds". *Systems and Control Letters*, 9, pp. 423–431, 1987.

[14] W. M. Haddad and D. S. Bernstein. "Robust Reduced-Order Modeling Via the Optimal Projection Equations with Petersen-Hollot Bounds". *IEEE Trans. on Auto. Control*, 33(7), pp. 692–694, July 1988.

[15] W. M. Haddad and D. S. Bernstein. "Robust, Reduced-Order, Nonstrictly Proper State Estimation Via the Optimal Projection Equations with Guaranteed Cost Bounds". *IEEE Trans. on Auto. Control*, 33(6), pp. 591–595, June 1988.

[16] W. M. Haddad and D. S. Bernstein. "Unified Optimal Projection Equations for Simultaneous Reduced-Order, Robust Modelling, Estimation, and Control". *Int. Journal of Control*, 47(4), pp. 1117–1132, 1988.

[17] C.V. Hollot and W.E. Schmitendorf. "Robust Stabilization of Tranfer Function Described by Interval Denominators and RHP Zeros". *Proc. 1989 Conference on Decision and Control, Tampa, FL*, pp. 1703–1704, December 1989.

[18] C.V. Hollot and F. Yang. "Robust Stabilization of Interval Plants Using Lead or Lag Compensators". *Proc. 1989 Conference on Decision and Control, Tampa, FL*, pp. 43–45, December 1989.

[19] H. Kwakernaak and R. Sivan. *Linear Optimal Control Systems.* Wiley-Interscience, 1972.

[20] M. Mansour. "Robust Stability of Interval Matrices". *Proc. 1989 Conference on Decision and Control, Tampa, FL*, pp. 46–51, December 1989.

[21] R.J. Minnichelli, I.J. Anagnost, and C.A. Desoer. "An Elementary Proof of Kharitonov's Stability Theorem with Extensions". *IEEE Trans. on Auto. Control*, 34(9), pp. 995–998, September 1989.

[22] D. Obradovic. *Design of a Robust Control System for Postfailure Operation.* PhD thesis, Massachusetts Institute of Technology, June 1990.

[23] I. R. Petersen. "A Stabilization Algorithm for a Class of Uncertain Linear Systems". *Systems and Control Letters*, 8, pp. 351–357, 1987.

[24] I. R. Petersen. "Disturbance Attenuation and H^∞ Optimization: A Design Method Based on The Algebraic Riccati Equation". *IEEE Trans. on Auto. Control*, 32(5), pp. 427–429, May 1987.

[25] I. R. Petersen. "Some New Results on Algebraic Riccati Equations arising in Linear Quadratic Differential Games and the Stabilization of Uncertain Linear Systems". *Systems and Control Letters*, 10, pp. 341–348, 1988.

[26] I. R. Petersen. "A Class of Stability Regions for Which a Kharitonov-Like Theorem Holds". *IEEE Trans. on Auto. Control*, 34(10), pp. 1111–1115, October 1989.

[27] I. R. Petersen. "A New Extenstion to Kharitonov's Theorem". *IEEE Trans. on Auto. Control*, 35(7), pp. 825–828, July 1990.

[28] I. R. Petersen and C. V. Hollot. "A Riccati Equation Approach to the Stabilization of Uncertain Linear Systems". *Automatica*, 22(4), pp. 397–411, 1986.

[29] M. Safonov and M. Athans. "Gain and Phase Margins for Multiloop LQG Regulators". *IEEE Trans. on Auto. Control*, 22(2), pp. 173–179, April 1977.

[30] B. Wei and D. S. Bernstein. "A Benchmark Problem for Robust Control Design". *Proc. 1990 American Control Conference, San Diego, CA*, pp. 961–962, May 1990.

[31] K. Wei. "Quadratic Stabilizability of Linear Systems with Structural Independent Time-Varying Uncertainties". *IEEE Trans. on Auto. Control*, 35(3), pp. 268–277, March 1990.

[32] K.H. Wei and B.R. Barmish. "On Making a Polynomial Hurwitz Invariant by Choice of Feedback Gains". *Proc. 1985 Conference on Decision and Control, Ft. Lauderdale, FL*, pp. 679–685, December 1985.